Distributed Faulty Node Detection in Delay Tolerant Networks: Design and Analysis

Wenjie Li, Laura Galluccio, Francesca Bassi, Michel Kieffer

Distributed Faulty Node Detection in Delay Tolerant Networks: Design and Analysis

Wenjie Li, *Student Member, IEEE,* Laura Galluccio, *Member, IEEE,*
Francesca Bassi, *Member, IEEE,* and Michel Kieffer, *Senior Member, IEEE*

Abstract—Propagation of faulty data in Delay Tolerant Networks can be a critical aspect to counteract due to the inherent feature of exhibiting frequent disconnections,. Indeed the rare meeting events require that nodes are effective and efficient in propagating correct information. Accordingly, mechanisms to rapidly identify possible faulty or misbehaving nodes should be searched. Distributed fault detection has been addressed in the literature in the context of sensor and vehicular networks, but already proposed solutions suffer from long delays in identifying and isolating misbehaving nodes. This paper proposes a fully distributed, easily implementable, and fast convergent approach to allow each DTN node to rapidly identify whether its sensors are producing outliers, *i.e.*, fauty data. The behavior of the proposed algorithm is described by some continuous-time state equations, whose equilibrium is characterized. Detection and false alarm rates are estimated by comparing both theoretical and simulation results. Numerical results assess the effectiveness of the proposed solution and give guidelines in the design of the algorithm.

Index Terms—Delay tolerant network; Fault detection; Iterative algorithms; Distributed estimation; State equations; Equilibrium analysis.

1 Introduction

Delay/Disruption-Tolerant Networks (DTN) are challenging networks which have dynamic topology with frequent disconnectivity [1]. For example, in Vehicular DTNs (VDTNs) [2], two nodes can communicate with each other only when they are closely located. This connection is intermittent as the nodes are moving vehicles. Due to this sparse and intermittent connectivity, inference and learning over DTNs is much more complicated than in traditional networks, see, *e.g.*, [3]–[7].

This paper considers the problem of distributed defective node detection in DTNs. A node is considered as defective when one of its sensors frequently reports erroneous measurements. The identification of such defective nodes is very important to save communication resources and to prevent erroneous measurements polluting estimates provided by the DTN. We assume, as in [8], that nodes are not aware of the status (good or defective) of their sensors, while their computation and communication capabilities remain fine, even if some of their sensors are defective. Moreover, each node of the DTN is assumed to behave in a rational way and is willing to know the status of its sensors.

Distributed fault detection (DFD) is a well-investigated topic when considering Wireless Sensor Networks (WSNs), see [9]–[11] and references therein. The WSNs considered in most of the literature are dense and have a static topology. DFD in DTNs is much less investigated. Classical DFD algorithms usually consist of two phases. First, a local outlier detection test (LODT) is performed using data collected from neighboring nodes. LODTs (based on majority voting [12], the median [13], or the mean [14] of the measurements, the modified three-sigma edit test [15], *etc*.) aim to decide which data is erroneous. Second, the outcomes of the LODTs are disseminated to improve the decision accuracy. When only few measurements are available, classical LODTs are not very efficient: for example, they cannot, based on two measurements only, determine which node is defective. This is a typical situation in DTNs when two nodes meet, take measurements, and share these measurements. Applying directly classical DFD algorithms in DTNs may thus be quite ineffective. Moreover, usually the performance of DFD algorithms is characterized experimentally. Theoretical analysis of the equilibrium and convergence properties of these algorithms is seldom performed.

A closely related problem has been previously considered in [16] in the context of VDTN. A large number of sensor nodes are fixed and some vehicles, called mobile carriers (MC) collect data from these sensors. The sensor nodes can only communicate with the MCs in their vicinity. A MC needs to collect enough measurements to perform a test to decide which have been produced by defective sensors. Once a defective node is deemed defective by a MC, it is added to its blacklist. The MC provides information to sensors about their status. MCs also exchange their blacklists to accelerate the faulty node detection.

In [17], a similar problem of distributed malware detection in DTN is addressed. Each node evaluates after the meeting with another node whether the latter has performed suspicious actions (malware transmission trial). When after several meetings of Node j, Node i detects

- *W. Li, F. Bassi, and M. Kieffer are with Laboratoire des Signaux et Systèmes (L2S, UMR CNRS 8506) CNRS-CentraleSupelec-Université Paris-Sud 3, rue Joliot Curie 91192 Gif-sur-Yvette, France. E-mail: firstname.name@lss.supelec.fr*
- *L. Galluccio is with Dipartimento di Ingegneria Elettrica, Elettronica e Informatica, University of Catania, 95125 Catania, Italy. E-mail: lauragalluccio@gmail.com*
- *M. Kieffer is also with LTCI Telecom ParisTech, 75013 Paris, France and Institut Universitaire de France, 75005 Paris, France*
- *F. Bassi is also with ESME-Sudria, 94200 Ivry-sur-Seine, France*

often suspicious activities, a cut-off decision is performed against Node j, which is ignored in next meetings. The main drawback of this approach is the long time required to identify and isolate misbehaving nodes. Misbehavior detection in DTN is also considered in [5], [18], where the DTN is perturbed by routing misbehavior caused by selfish or malicious nodes. The identification approach in [5] is not distributed, since a Trusted Authority periodically checks the forwarding history of nodes to identify possible misbehavior. A collaborative approach is proposed in [18], where each node can detect whether the encountered node is selfish using a local watchdog. The detection result is disseminated over the network to increase the detection precision and to reduce the delay. Trust/Reputation managemement is another important aspect to help DTNs resist various potential threats. For example, [19] provides an iterative trust management mechanism to fight against Byzantine attacks in which several nodes are totally controlled by the adversary. In [20], a defense against Sybil attacks [21] is introduced, which is based on the physical feature of the wireless propagation channel. A trust model for underwater acoustic sensor networks is presented in [22] to take into account several trust metrics such as link trust, data trust, and node trust.

This paper presents a fully distributed and easily implementable algorithm to allow each node of a DTN to determine whether its own sensors are defective. As in [8], a LODT is assumed to be able to detect the presence of outliers in a set of measurements, without necessarily being able to determine which are the outliers. The generic LODT is characterized by its probabilities of detection and of false alarm. When two nodes meet, they exchange their local measurements and use them to perform the same LODT. The LODT results help both nodes to update their estimate of the status of their own sensors. When, for a given node, the proportion of meetings during which the LODT suggests the presence of outliers is larger than some threshold, this node decides its sensors may be defective. In this case, it becomes silent. It does not transmit any more its measurements to its neighbors, but keeps collecting measurements from nodes met and updating the estimate of the status of its sensors. It may then have the opportunity to update its estimate and to communicate again. Although the LODT considered here are those of [8], this work differs significantly from [8] due to the communication conditions of DTNs, which require a totally different DFD algorithm. The analysis of the properties of the algorithm is also totally different. This paper shows that the behavior of the proposed DFD algorithm can be analyzed using Markov models and tools borrowed from control theory and population dynamics. For that purpose, the belief of each node about the status of its sensors is quantized. The evolution of these quantized beliefs are then shown to follow two Markov chains. The dynamic of the proportions of nodes with a given belief is then analyzed. Sufficient conditions on the decision parameters to ensure the existence and unicity of an equilibrium of the DFD algorithm are then provided. Given the characteristics of the LODT, upper and lower bounds of the *detection rate*, *i.e.*, proportion of nodes which have effectively identified their sensors as defective, and of the *false alarm rate*, *i.e.*, proportion of nodes which believe that their good sensors are in fact defective, are also obtained. These theoretical results provide guidelines to properly choose the parameters of the algorithm.

TABLE 1
Symbols used in this paper

θ_i	status of the sensors of Node i
$\widehat{\theta}_i$	estimate of status of the sensors of Node i
λ	inter-contact rate
ν	decision threshold
t	time instant
y_i	outcome of a LODT performed by Node i
q_{D}	detection probability of a LODT
q_{FA}	false alarm probability of a LODT
$c_{\mathrm{m},i}$	number of LODTs performed by Node i
$c_{\mathrm{d},i}$	number of LODTs by Node i resulting in a detection of outliers
M	window size of the LODT results that are considered for the decision
$\mathbf{x}_i$	state of Node i, containing θ_i, $c_{\mathrm{m},i}$, and $c_{\mathrm{d},i}$
$X_\theta^{\ell,k}$	state component of the DTN: proportion of nodes in state $\mathbf{x}_i = (\theta, \ell, k)$ among the nodes with sensors of actual status θ
p_θ	proportion of nodes with sensors of status θ
$p^{\theta\widehat{\theta}}$	proportion of nodes believing its sensors are in status $\widehat{\theta}$, among the nodes with sensors of actual status θ
$\overline{X}_\theta^{\ell,k}$	value of $X_\theta^{\ell,k}$ at equilibrium
$\overline{p}^{\theta\widehat{\theta}}$	value of $p^{\theta\widehat{\theta}}$ at equilibrium
$\widetilde{X}_\theta^{\ell,k}$	approximate value of $X_\theta^{\ell,k}$ at equilibrium
$\widetilde{p}^{\theta\widehat{\theta}}$	approximate value of $p^{\theta\widehat{\theta}}$ at equilibrium

The rest of the paper is organized as follows. Section 2 presents the system model and basic assumptions. Section 3 details the DFD algorithm for DTNs. Section 4 discusses the transition probabilities between the state values for some reference nodes. Section 5 develops the theoretical analysis of the macroscopic evolution of the proportion of nodes in different states. Section 6 analyzes the property of the equilibrium obtained from the state equations. Section 7 presents the approximation of the proportion of nodes at the equilibrium and discusses the choice of the parameters in the algorithm. Section 8 provides some numerical results and Section 9 concludes this paper. Notations are presented in Table 1.

2 System Model

Consider a set $\mathcal{S}$ of N_S moving nodes equipped with sensors. $\mathcal{D} \subset \mathcal{S}$ represents the subset of nodes with defective sensors producing *outliers*, *i.e.*, measurements corrupted by a noise which has characteristics significantly different from those of the noise corrupting measurements provided by good sensors. The *status* of Node i is $\theta_i(t) = 0$ (good node) if all its sensors are good and $\theta_i(t) = 1$ (defective node) if at least one of them is defective. The proportion of nodes with good and defective status are p_0 and p_1, with $p_0 + p_1 = 1$. Each node is not aware of its own status. In what follows, we assume that over the time horizon of the experiment, the status of sensors does not change, *i.e.*, $\theta_i(t) = \theta_i$.

Our aim is (*i*) to design a distributed algorithm so that each Node i rapidly evaluates an accurate estimate $\widehat{\theta}_i$ of its own status θ_i, as fast as possible, (*ii*) to provide a theoretical analysis of the behavior of this algorithm.

2.1 Communication model

Nodes can exchange information only during the limited time interval in which they are in vicinity. As in [6], [7], [18], [23], we assume that the time interval between two successive meetings follows an exponential distribution with an inter-contact rate λ. Moreover, we assume that each meeting involves only two nodes. When more than two nodes meet at the same time instant, processing is performed pair-by-pair. These assumptions facilitate the analysis of the proposed DFD algorithm.

2.2 Local outlier detection test

As in [8], we consider a family of LODTs able to detect the presence of outliers in a set of n data (measurements, measurements with associated regressors or experimental conditions) $\mathcal{M} = \{m_1, \ldots, m_n\}$ but unable to identify which data is an outlier. Denote $y(\mathcal{M})$ the outcome of the LODT, *i.e.*, $y(\mathcal{M}) = 1$ if data corresponding to outlier are detected within $\mathcal{M}$, otherwise, $y(\mathcal{M}) = 0$.

LODTs can take various forms, see [8] and Example 1 below. The LODT is characterized by a false alarm probability q_{FA} (the probability of having $y(\mathcal{M}) = 1$ under the condition that none of the data in $\mathcal{M}$ are produced by defective sensors) and by a detection probability q_{D} (the probability of having $y(\mathcal{M}) = 1$ under the condition that some data in $\mathcal{M}$ are really produced by some defective sensors). Let n_0 be the number of data produced by good sensors and n_1 be the number of data coming from defective sensors. We further assume that both q_{D} and q_{FA} depend on the number of data involved in the LODT. As a consequence, we can denote q_{FA} as $q_{\text{FA}}(n_0)$ and q_{D} as $q_{\text{D}}(n_0, n_1)$. Each node performing a LODT on a set of data has not to know n_0 and n_1, but the performance of the LODT will depend on the actual values of n_0 and n_1, which are used in the analysis of the DFD algorithm.

Example 1. This example introduces a LODT suited to a DTN aiming at solving a bounded-error parameter estimation problem, see, *e.g.*, [24]–[26]. In such a context, some parameter vector has to be estimated from noisy measurements. The noise corrupting the measurements provided by good sensors is assumed bounded with known bounds. Let $\mathbf{x} \in \mathcal{X} \subset \mathbb{R}^{n_{\text{x}}}$ be the vector of parameters to be estimated from the vector measurements $\mathbf{z}_1, \ldots, \mathbf{z}_{n_{\text{s}}}$ provided by n_{s} sensors. Here, the data m_i is a vector measurement $\mathbf{z}_i$. Assume that the measurement model is

$$\mathbf{z}_i = \mathbf{z}_{\text{m}}(\mathbf{x}^*) + \mathbf{w}_i \tag{1}$$

where $\mathbf{x}^*$ is the true value of the parameter vector, $\mathbf{z}_{\text{m}}$ is a possibly non-linear model of the measurement process, and $\mathbf{w}_i$ is some noise such that $\|\mathbf{w}_i\|_\infty \leqslant \varepsilon$, with ε representing some known noise bound. One may then introduce the set $\mathbb{X}_i$ of parameter vectors *consistent* with measurement $\mathbf{z}_i$ as

$$\mathbb{X}_i = \left\{\mathbf{x} \in \mathcal{X} \,|\, \|\mathbf{z}_i - \mathbf{z}_{\text{m}}(\mathbf{x})\|_\infty \leqslant \varepsilon\right\} \tag{2}$$

and the set $\mathbb{X}$ of parameter vectors *consistent* with *all measurements* as

$$\mathbb{X} = \bigcap_{i=1}^{n_{\text{s}}} \mathbb{X}_i = \left\{\mathbf{x} \in \mathcal{X} \,|\, \|\mathbf{z}_i - \mathbf{z}_{\text{m}}(\mathbf{x})\|_\infty \leqslant \varepsilon, i = 1 \ldots n_{\text{s}}\right\}. \tag{3}$$

Accurate inner and outer-approximations of $\mathbb{X}$ may be obtained, even for models $\mathbf{z}_{\text{m}}$ non-linear in $\mathbf{x}$ with ellipsoids, parallelotopes, zonotopes, boxes, unions of boxes, see [26], [27]. When $\mathbb{X}$ is empty, the model $\mathbf{z}_{\text{m}}$ is either not suited to describe the system of interest, or the bounded noise property $\|\mathbf{w}_i\|_\infty \leqslant \varepsilon$ is not satisfied for at least one measurement, *i.e.*, there is at least one defective sensor. An empty $\mathbb{X}$ may be obtained even with as few as two vector measurements, providing the ability to detect outliers with very few sensor readings. A LODT may then be designed in such bounded-error parameter estimation context considering a set of measurements $\mathbf{z}_1 \ldots \mathbf{z}_{n_{\text{s}}}$ by checking whether the set $\mathbb{X}$ introduced in (3) is empty or not.

2.3 Detection scenario

We assume that during each meeting of a pair of nodes $(i, j) \in \mathcal{S}$, the nodes collect data with their sensors. Each node may or may not transmit its data to the other node. If a node has received data from its neighbor, it may run a LODT involving its own data and those received from its neighbor. We assume that the spatial and temporal correlation between data is such that only data collected during the meeting of two nodes can be exploited by a LODT. Therefore, previously collected data are not exploited. As a consequence, contrary to [8], where n_0 and n_1 may be large, in the DTN scenario, a LODT will involve $n_0, n_1 \in \{0, 1, 2\}$, with $n_0 + n_1 = 2$. In this paper, one furthermore assumes that $q_{\text{FA}}(2) < q_{\text{D}}(1, 1) \leqslant q_{\text{D}}(0, 2)$, which is reasonable, since the outcome of a LODT is more likely to be 1 as the number of outliers involved increases.

3 DFD ALGORITHM

In the proposed DFD algorithm, each node manages two counters $c_{\text{m},i}(t)$ and $c_{\text{d},i}(t)$ initialized at 0 at $t = 0$. Using $c_{\text{m},i}(t)$, Node i counts the number of *meetings* during which it has received data from its neighbor, and has been able to perform a LODT. Using $c_{\text{d},i}(t)$, it counts the number of LODT tests resulting in the *detection* of outliers. When $c_{\text{d},i}(t)/c_{\text{m},i}(t) \geqslant \nu$, where ν is some constant decision threshold, Node i considers itself as carrying defective sensors, *i.e.*, it sets its own estimate $\widehat{\theta}_i(t) = 1$. Otherwise, it considers that its sensors are good, *i.e.*, $\widehat{\theta}_i(t) = 0$.

When a node with $\widehat{\theta}_i(t) = 1$ encounters another node, it still takes measurements, but it does not send these data to the other node to avoid infecting the network with outliers. Any node, upon receiving data from another node, performs a LODT and updates $c_{\text{m},i}(t)$ and $c_{\text{d},i}(t)$. As a consequence, a node which meets another node considering itself as defective, transmits its data, but since it does not receive any data, it does not update $c_{\text{m},i}(t)$ and $c_{\text{d},i}(t)$ at the end of the meeting. Algorithm 1 summarizes the proposed DFD technique for an arbitrary reference Node i.

The vector $\mathbf{x}_i(t) = (\theta_i, c_{\text{m},i}(t), c_{\text{d},i}(t))$ represents the (microscopic) *state* of each *Node* i. As $t \to \infty$, one has $c_{\text{m},i}(t) \to \infty$, which leads to an infinite number of possible values for $\mathbf{x}_i(t)$ and the global (macroscopic) behavior of the algorithm is difficult to analyze. To limit the number of possible states, one has chosen to consider the evolution of $c_{\text{m},i}(t)$ and $c_{\text{d},i}(t)$ over a sliding time window containing the time instants of the last M meetings during which Node i has performed a LODT. Algorithm 2 is a modified version of Algorithm 1 accounting for this limited horizon procedure.

Algorithm 1 DFD algorithm for Node i

1) Initialize at $t_i^0 = 0$, $\widehat{\theta}_i\left(t_i^0\right) = 0$, $c_{\mathrm{m},i}(t_i^0) = c_{\mathrm{d},i}(t_i^0) = 0$, $\kappa = 1$.
2) Do

$$\begin{cases} \widehat{\theta}_i\left(t\right) = \widehat{\theta}_i\left(t_i^{\kappa-1}\right), \\ c_{\mathrm{m},i}\left(t\right) = c_{\mathrm{m},i}\left(t_i^{\kappa-1}\right), \\ c_{\mathrm{d},i}\left(t\right) = c_{\mathrm{d},i}\left(t_i^{\kappa-1}\right), \end{cases} \tag{4}$$

$$t = t + \delta t \tag{5}$$

until the κ-th meeting occurs at time $t = t_i^\kappa$ with Node $j^\kappa \in \mathcal{S} \setminus \{i\}$.
3) Perform local measurement of data $m_i\left(t_i^\kappa\right)$.
4) If $\widehat{\theta}_i\left(t_i^\kappa\right) = 0$, then transmit $m_i\left(t_i^\kappa\right)$ to Node j^κ.
5) If data m_{j^κ} have been received from Node j^κ, then
   a) Perform a LODT with outcome $y_i\left(t_i^\kappa\right)$.
   b) Update $c_{\mathrm{m},i}$ and $c_{\mathrm{d},i}$ according to

$$\begin{cases} c_{\mathrm{m},i}(t_i^\kappa) = c_{\mathrm{m},i}(t_i^{\kappa-1}) + 1 \\ c_{\mathrm{d},i}(t_i^\kappa) = c_{\mathrm{d},i}(t_i^{\kappa-1}) + y_i\left(t_i^\kappa\right) \end{cases} \tag{6}$$

   c) Update $\widehat{\theta}_i$ as follows

$$\widehat{\theta}_i(t_i^\kappa) = \begin{cases} 1 & \text{if } c_{\mathrm{d},i}(t_i^\kappa)/c_{\mathrm{m},i}(t_i^\kappa) \geqslant \nu, \\ 0 & \text{else.} \end{cases} \tag{7}$$

6) $\kappa = \kappa + 1$.
7) Go to 2.

It involves an additional counter μ indicating the number of LODT performed by Node i. Note that when $\mu < M$, then (8) is equivalent to (6).

The next sections are devoted to the analysis of Algorithm 2.

Algorithm 2 Sliding-Window DFD algorithm for Node i

1) Initialize $t_i^0 = 0$, $\widehat{\theta}_i\left(t_i^0\right) = 0$, $c_{\mathrm{m},i}(t_i^0) = c_{\mathrm{d},i}(t_i^0) = 0$, $\kappa = 1$, and $\mu = 0$.
2) Do (4)-(5) until the κ-th meeting occurs at time t_i^κ with Node $j^\kappa \in \mathcal{S} \setminus \{i\}$.
3) Perform local measurement of data $m_i\left(t_i^\kappa\right)$.
4) If $\widehat{\theta}_i\left(t_i^\kappa\right) = 0$, then transmit $m_i\left(t_i^\kappa\right)$ to Node j^κ.
5) If data m_{j^κ} have been received from Node j^κ, then
   a) $\mu = \mu + 1$. Perform a LODT with outcome y_i^μ.
   b) Update $c_{\mathrm{m},i}$ and $c_{\mathrm{d},i}$ as

$$\begin{cases} c_{\mathrm{m},i}(t_i^\kappa) = \min\left\{\mu, M\right\}, \\ c_{\mathrm{d},i}(t_i^\kappa) = \sum_{m=\max\{1,\mu-M+1\}}^{\mu} y_i^m. \end{cases} \tag{8}$$

   c) Update $\widehat{\theta}_i$ using (7).

6) $\kappa = \kappa + 1$.
7) Go to 2.

4 Evolution of the State of a Node

The state of Node i is represented by the triple $\mathbf{x}_i(t) = (\theta, c_{\mathrm{m},i}\left(t\right), c_{\mathrm{d},i}\left(t\right))$. Since $c_{\mathrm{m},i}\left(t\right) \in \{0, 1 \dots M\}$ and $c_{\mathrm{d},i}\left(t\right) \in \{0 \dots c_{\mathrm{m},i}\left(t\right)\}$, the number of values that may be taken by the state of a node is $\sum_{\ell=0}^{M}(\ell+1) = (M+1)(M+2)/2$. The evolution of the state of Node i, conditioned by its status θ_i, follows a Markov model with state transition diagram similar to that shown in Figure 1 for $M = 4$.

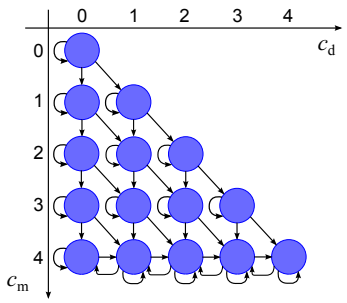

Fig. 1. Example of Markov model for the evolution of the state of a node when $M = 4$.

In particular, there are two chains, one conditioned by $\theta_i = 0$ and the other conditioned by $\theta_i = 1$. Both are characterized by a transient phase for state values with $c_{\mathrm{m},i}(t) < M$, then, a permanent regime starts when $c_{\mathrm{m},i}(t) = M$. With $c_{\mathrm{m},i}\left(t\right) = \ell$ and $c_{\mathrm{d},i}\left(t\right) = k$, the transitions from State (θ, ℓ, k) to State (θ, ℓ', k') are analyzed in what follows.

Assume that the reference Node i meets a random Node J at time t and define the random event

$$\mathcal{E}_1(t) = \left\{\widehat{\theta}_J\left(t\right) = 0\right\}, \tag{9}$$

representing the event that the node met believes its status is good. According to (7), among the nodes with status θ, the proportion of nodes that believe themselves as good is [1]

$$p^{\theta 0}\left(t\right) = X_\theta^{0,0}\left(t\right) + \sum_{\ell,k,k/\ell<\nu} X_\theta^{\ell,k}\left(t\right), \tag{10}$$

where $p^{10}\left(t\right)$ is in fact the *non-detection rate* (NDR) of the nodes with defective sensors at time t. Assuming that the nodes are randomly spread, the probability that Node J believes it has only good sensors conditioned to its true status is

$$\mathbb{P}\left(\widehat{\theta}_J\left(t\right) = 0 | \theta_J\left(t\right) = \theta\right) = p^{\theta 0}\left(t\right), \tag{11}$$

and then

$$\mathbb{P}\left\{\mathcal{E}_1(t)\right\} = p_0 p^{00}\left(t\right) + p_1 p^{10}\left(t\right). \tag{12}$$

Similarly, introducing $\overline{\mathcal{E}_1}(t) = \{\widehat{\theta}_J\left(t\right) = 1\}$, among the nodes with sensors in status θ, the proportion of nodes with $\widehat{\theta}_j\left(t\right) = 1$ is

$$p^{\theta 1}\left(t\right) = \sum_{\ell,k,k/\ell\geqslant\nu} X_\theta^{\ell,k}\left(t\right), \tag{13}$$

where $p^{01}\left(t\right)$ and $p^{11}\left(t\right)$ represent the *false alarm rate* (FAR) and the *detection rate* (DR) respectively. From (13), one gets

$$\mathbb{P}\left\{\overline{\mathcal{E}_1}(t)\right\} = p_0 p^{01}\left(t\right) + p_1 p^{11}\left(t\right). \tag{14}$$

Since Node i performs an LODT only when it meets a node J with $\widehat{\theta}_J\left(t\right) = 0$, one introduces the random event

$$\mathcal{E}_2^\theta(t) = \left\{Y_i\left(t\right) = 1 \mid \theta_i = \theta, \widehat{\theta}_J\left(t\right) = 0\right\}, \tag{15}$$

1. For the sake of simplicity, the dependency of $p^{\theta 0}\left(t\right)$ in ν is omitted, as ν is constant during the DFD algorithm.

for the reference node with actual status θ. As detailed in Section 2.2, the statistical properties of the outcome $Y_i(t)$ of the LODT depend only on θ_i and θ_j. For example, when Node i has good sensors, one has

$$\begin{aligned}\mathbb{P}\left\{\mathcal{E}_2^0(t)\right\} &= \sum_{\varphi=0}^{1}\mathbb{P}\left\{Y_i(t)=1,\theta_J=\varphi \mid \theta_i=0,\widehat{\theta}_J(t)=0\right\}\\ &\overset{(a)}{=} \sum_{\varphi=0}^{1}\mathbb{P}\left\{Y_i(t)=1 \mid \theta_i=0,\theta_J=\varphi\right\}\mathbb{P}\left\{\theta_J=\varphi \mid \widehat{\theta}_J(t)=0\right\}\\ &\overset{(b)}{=} \frac{p_0 q_{\mathrm{FA}}(2)\,p^{00}(t)+p_1 q_{\mathrm{D}}(1,1)\,p^{10}(t)}{p_0 p^{00}(t)+p_1 p^{10}(t)}. \end{aligned} \tag{16}$$

In (16-a), one uses the fact that the LODT outcome is not influenced by the estimate of the status of a node and that in $\mathbb{P}\left\{\theta_J=\varphi \mid \theta_i=0,\widehat{\theta}_J(t)=0\right\}$, the status of Node J, does not depend on θ_i. In (16-b),

$$\begin{cases}\mathbb{P}\left\{Y_i(t)=1 \mid \theta_i=0,\theta_J=0\right\}=q_{\mathrm{FA}}(2),\\ \mathbb{P}\left\{Y_i(t)=1 \mid \theta_i=0,\theta_J=1\right\}=q_{\mathrm{D}}(1,1).\end{cases} \tag{17}$$

Moreover,

$$\begin{aligned}&\mathbb{P}\left\{\theta_J=\varphi \mid \widehat{\theta}_J(t)=0\right\}\\ &=\frac{\mathbb{P}\left\{\widehat{\theta}_J(t)=0|\theta_J=\varphi\right\}\mathbb{P}\{\theta_J=\varphi\}}{\sum_{\phi=0}^{1}\mathbb{P}\left\{\widehat{\theta}_J(t)=0|\theta_J=\phi\right\}\mathbb{P}\{\theta_J=\phi\}}=\frac{p_\varphi p^{\varphi 0}(t)}{p_0p^{00}(t)+p_1p^{10}(t)}.\end{aligned}$$

Now, if Node i has defective sensors, (15) can be expressed as

$$\mathbb{P}\left\{\mathcal{E}_2^1(t)\right\}=\frac{p_0 q_{\mathrm{D}}(1,1)\,p^{00}(t)+p_1 q_{\mathrm{D}}(0,2)\,p^{10}(t)}{p_0p^{00}(t)+p_1p^{10}(t)}. \tag{18}$$

Similarly, one may introduce the random event

$$\mathcal{E}_3^\theta(t)=\left\{Y_i(t)=0 \mid \theta_i=\theta,\widehat{\theta}_J(t)=0\right\}, \tag{19}$$

and show that

$$\begin{aligned}&\mathbb{P}\left\{\mathcal{E}_3^\theta(t)\right\}\\ &=\begin{cases}\frac{p_0(1-q_{\mathrm{FA}}(2))p^{00}(t)+p_1(1-q_{\mathrm{D}}(1,1))p^{10}(t)}{p_0p^{00}(t)+p_1p^{10}(t)}, & \text{if } \theta=0,\\ \frac{p_0(1-q_{\mathrm{D}}(1,1))p^{00}(t)+p_1(1-q_{\mathrm{D}}(0,2))p^{10}(t)}{p_0p^{00}(t)+p_1p^{10}(t)}, & \text{if } \theta=1.\end{cases}\end{aligned} \tag{20}$$

Define $\pi_\theta^{\delta_{\mathrm{m}},\delta_{\mathrm{d}}}$ as the transition probability from State (θ,ℓ,k) to State $(\theta,\ell+\delta_{\mathrm{m}},k+\delta_{\mathrm{d}})$, where $\theta\in\{0,1\}$. One has $\delta_{\mathrm{m}}\in\{0,1\}$ since ℓ may either increase $(\delta_{\mathrm{m}}=1)$ in the transient regime or remain constant $(\delta_{\mathrm{m}}=0)$ in the permanent regime. One has $\delta_{\mathrm{d}}\in\{-1,0,1\}$, depending on the value of the last LODT outcome and on the value of the $M+1$-th last LODT outcome, which is no more considered in the permanent regime. Thus, $(\delta_{\mathrm{m}},\delta_{\mathrm{d}})\in\{(0,0),(0,1),(0,-1)(1,0),(1,1),(1,-1)\}$. Note that $\pi_\theta^{\delta_{\mathrm{m}},\delta_{\mathrm{d}}}$ depends on the current state of the reference node, but also on the current proportion of active (good and defective) nodes. Therefore, the transition probabilities are denoted as $\pi_\theta^{\delta_{\mathrm{m}},\delta_{\mathrm{d}}}(t,\ell,k)$, where t is the time instant, $c_{\mathrm{m},i}(t)=\ell$, and $c_{\mathrm{d},i}(t)=k$. Depending on the value of ℓ, two different cases are considered in Section 4.1 and in Section 4.2, respectively corresponding to the transient and permanent regimes.

4.1 Case I, $\ell < M$

In the transient regime, when $c_{\mathrm{m},i}(t)=\ell<M$, $c_{\mathrm{m},i}(t)$ and $c_{\mathrm{d},i}(t)$ are updated according to (6) whenever Node J with $\widehat{\theta}_J(t)=0$ is met,. The only possibility that leads to $\delta_{\mathrm{m}}=0$ is the event $\overline{\mathcal{E}_1}$, *i.e.*, Node i meets Node J with $\widehat{\theta}_J(t)=1$. As a consequence, no LODT is performed by Node i. Therefore, for any $\theta\in\{0,1\}$,

$$\pi_\theta^{0,0}(t,\ell,k)=\mathbb{P}\left\{\overline{\mathcal{E}_1}(t)\right\}=p_0p^{01}(t)+p_1p^{11}(t), \tag{21}$$

where $p^{\theta 1}(t)$ is defined by (13).

A state transition occurs with $(\delta_{\mathrm{m}},\delta_{\mathrm{d}})=(1,1)$ when Node i with status $\theta_i=\theta$ meets Node J with $\widehat{\theta}_J(t)=0$ *and* when the LODT yields $y_i(t)=1$. Since the two events are independent, one has

$$\begin{aligned}\pi_\theta^{1,1}(t,\ell,k)&=\mathbb{P}\left\{Y_i(t)=1,\widehat{\theta}_J(t)=0|\theta_i=\theta\right\}\\ &=\mathbb{P}\left\{\mathcal{E}_1(t)\right\}\mathbb{P}\left\{\mathcal{E}_2^\theta(t)\right\}.\end{aligned} \tag{22}$$

Depending on the value of θ_i, using (12), (16), and (18), one may rewrite (22) as

$$\pi_\theta^{1,1}(t,\ell,k)=\begin{cases}p_0q_{\mathrm{FA}}(2)\,p^{00}(t)+p_1q_{\mathrm{D}}(1,1)\,p^{10}(t), & \text{if } \theta=0,\\ p_0q_{\mathrm{D}}(1,1)\,p^{00}(t)+p_1q_{\mathrm{D}}(0,2)\,p^{10}(t), & \text{if } \theta=1.\end{cases} \tag{23}$$

Finally, $\pi_\theta^{1,0}(t,\ell,k)=\mathbb{P}\left\{Y_i(t)=0,\widehat{\theta}_J(t)=0|\theta_i=\theta\right\}$ is obtained similarly from (20)

$$\pi_\theta^{1,0}(t,\ell,k)=\begin{cases}p_0\left(1-q_{\mathrm{FA}}(2)\right)p^{00}(t)+p_1\left(1-q_{\mathrm{D}}(1,1)\right)p^{10}(t), & \text{if } \theta=0,\\ p_0\left(1-q_{\mathrm{D}}(1,1)\right)p^{00}(t)+p_1\left(1-q_{\mathrm{D}}(0,2)\right)p^{10}(t), & \text{if } \theta=1.\end{cases} \tag{24}$$

4.2 Case II, $c_{\mathbf{m},i}(t)=M$

In the permanent regime, $c_{\mathrm{m},i}(t)=M$ and does not increase any more, thus $\delta_{\mathrm{m}}=0$. In Algorithm 2, μ is the number of LODTs performed by Node i up to time t. When $\mu\geqslant M$, only the last M LODT outcomes are considered: LODT outcomes y_i^m with $m\leqslant\mu-M$ are no more considered.

To determine the value taken by $\delta_{\mathrm{d}}\in\{-1,0,1\}$ after the μ-th LODT, consider the random event

$$\mathcal{E}_4^1(t)=\left\{Y_i^{\mu-M}=1 \mid \sum_{m=\mu-M}^{\mu-1}Y_i^m=k\right\}, \tag{25}$$

which corresponds to a situation where one knows that k LODTs where positive among the last M tests and the LODT that will be ignored, once the new LODT outcome is available, also concluded in the presence of defective sensors. $\mathbb{P}\left\{\mathcal{E}_4^1(t)\right\}$ is relatively complex to evaluate, since $\mathbb{P}\{Y_i^n=1\}$ is time-varying according to (16-18). In what follows, we assume that LODT outcomes with $Y_i^m=1$ are independently distributed over the time horizon corresponding to $m=\mu-M,\ldots,\mu-1$. One obtains then

$$\mathbb{P}\left\{\mathcal{E}_4^1(t)\right\}=\frac{k}{M}. \tag{26}$$

This approximation is exact in steady-state, when the $X_\theta^{\ell,k}$s do not vary any more. Similarly, define $\mathcal{E}_4^0(t)=\left\{Y_i^{\mu-M}=0 \mid \sum_{m=\mu-M}^{\mu-1}Y_i^m=k\right\}$. Making the same assumption used to get (26), one has

$$\mathbb{P}\left\{\mathcal{E}_4^0(t)\right\}=1-\mathbb{P}\left\{\mathcal{E}_4^1(t)\right\}\approx\frac{M-k}{M}. \tag{27}$$

Assume that the $(\mu - M)$-th LODT performed by Node i occurred at time $\tilde{t}$, then $y_i^{\mu-M}$ can also be denoted as $y_i(\tilde{t})$ and the transition related to $c_{\mathrm{d},i}$ is such that $\delta_{\mathrm{d}} = y_i(t) - y_i(\tilde{t}) \in \{-1, 0, 1\}$.

To have $(\delta_{\mathrm{m}}, \delta_{\mathrm{d}}) = (0, 1)$, three independent events have to occur: 1) the encountered Node J believes it is good at time t, *i.e.*, $\mathcal{E}_1(t)$; 2) $y_i(t) = 1$, *i.e.*, $\mathcal{E}_2(t)$; 3) $y_i(\tilde{t}) = 0$, *i.e.*, $\mathcal{E}_4^0(t)$. Thus the transition probability may be expressed as

$$\pi_\theta^{0,1}(t, M, k) = \mathbb{P}\{\mathcal{E}_1(t)\}\,\mathbb{P}\left\{\mathcal{E}_2^\theta(t)\right\}\mathbb{P}\{\mathcal{E}_4^0(t)\}. \quad (28)$$

Using (12), (16), (18), and (26) in (28), one gets

$$\pi_\theta^{0,1}(t, M, k) = \begin{cases} \left(p_0 q_{\mathrm{FA}}(2)\, p^{00}(t) + p_1 q_{\mathrm{D}}(1,1)\, p^{10}(t)\right)\frac{M-k}{M}, & \text{if } \theta = 0, \\ \left(p_0 q_{\mathrm{D}}(1,1)\, p^{00}(t) + p_1 q_{\mathrm{D}}(0,2)\, p^{10}(t)\right)\frac{M-k}{M}, & \text{if } \theta = 1. \end{cases} \quad (29)$$

Consider now $(\delta_{\mathrm{m}}, \delta_{\mathrm{d}}) = (0, -1)$. To have such transition, the three following independent events should occur: 1) $\mathcal{E}_1(t)$; 2) $y_i(t) = 0$, *i.e.*, $\mathcal{E}_3(t)$; 3) $y_i(\tilde{t}) = 1$, *i.e.*, $\mathcal{E}_4^1(t)$. Thus, the transition probability is

$$\pi_\theta^{0,-1}(t, M, k) = \mathbb{P}\{\mathcal{E}_1(t)\}\,\mathbb{P}\left\{\mathcal{E}_3^\theta(t)\right\}\mathbb{P}\{\mathcal{E}_4^1(t)\}$$
$$= \begin{cases} \left(p_0(1-q_{\mathrm{FA}}(2))\, p^{00}(t) + p_1(1-q_{\mathrm{D}}(1,1))\, p^{10}(t)\right)\frac{k}{M}, & \text{if } \theta = 0, \\ \left(p_0(1-q_{\mathrm{D}}(1,1))\, p^{00}(t) + p_1(1-q_{\mathrm{D}}(0,2))\, p^{10}(t)\right)\frac{k}{M}, & \text{if } \theta = 1. \end{cases} \quad (30)$$

Considering the last transition $(\delta_{\mathrm{m}}, \delta_{\mathrm{d}}) = (0, 0)$, to obtain the expression of $\pi_\theta^{0,0}(t, M, k)$, one needs to introduce (29-30) into

$$\pi_\theta^{0,0}(t, M, k) = 1 - \pi_\theta^{0,1}(t, M, k) - \pi_\theta^{0,-1}(t, M, k). \quad (31)$$

5 Macroscopic Evolution of the DTN State

At time t, among the nodes with status $\theta \in \{0, 1\}$, let $X_\theta^{\ell,k}(t)$ be the proportion of nodes in state (θ, ℓ, k). All node state transition probabilities evaluated in Section 4 are now used to determine the evolution of the *DTN state* components, *i.e.*, of the various proportions of nodes $X_0^{\ell,k}(t)$ and $X_1^{\ell,k}(t)$ in the corresponding states, with $\ell = 0, \ldots, M$ and $k \leqslant \ell$.

Considering an inter-contact rate λ and a well-mixed population of nodes, during a short time interval $[t, t + \delta t]$ the number of nodes with state (θ, ℓ, k) that will meet another node is $\lambda p_\theta N_S X_\theta^{\ell,k}(t)\delta t$.

When $0 < \ell < k < M$, these nodes will switch to the states $(\theta, \ell + \delta_{\mathrm{m}}, k + \delta_{\mathrm{d}})$, with $(\delta_{\mathrm{m}}, \delta_{\mathrm{d}}) \in \{(0,0), (1,0), (1,1)\}$ with a probability $\pi_\theta^{\delta_{\mathrm{m}},\delta_{\mathrm{d}}}(t, \ell, k)$. Moreover, nodes in the states $(\theta, \ell - 1, k - 1)$ and $(\theta, \ell - 1, k)$ that have met an other node in the time interval $[t, t + \delta t]$ may reach state (θ, ℓ, k), respectively with a probability $\pi_\theta^{1,1}(t, \ell - 1, k - 1)$ and $\pi_\theta^{1,0}(t, \ell - 1, k)$, see Figure 2.

As a consequence, at time $t + \delta t$, the number of nodes in State (θ, ℓ, k) may be expressed as follows

$$p_\theta N_S X_\theta^{\ell,k}(t + \delta t) = p_\theta N_S X_\theta^{\ell,k}(t) + \lambda \delta t p_\theta N_S \Big(-X_\theta^{\ell,k}(t)\left(\pi_\theta^{1,0}(t, \ell, k) + \pi_\theta^{1,1}(t, \ell, k)\right) + X_\theta^{\ell-1,k-1}(t)\pi_\theta^{1,1}(t, \ell-1, k-1) + X_\theta^{\ell-1,k}(t)\pi_\theta^{1,0}(t, \ell-1, k)\Big). \quad (32)$$

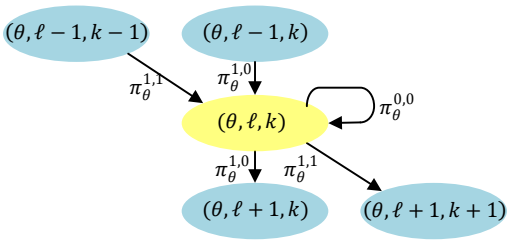

Fig. 2. Transient regime: Possible state transitions from and to state (θ, ℓ, k) when $0 < \ell < M$ and $0 < k < \ell$

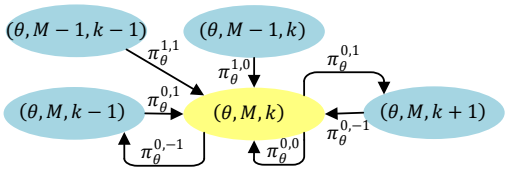

Fig. 3. Permanent regime: Possible state transitions from and to State (θ, M, k) when $0 < k < M$

The evolution of $X_\theta^{\ell,k}(t)$ is then described by the following differential equation, where the time dependency is omitted to lighten notations

$$\frac{dX_\theta^{\ell,k}}{dt} = -\lambda X_\theta^{\ell,k}\left(\pi_\theta^{1,0}(\ell, k) + \pi_\theta^{1,1}(\ell, k)\right) + \lambda X_\theta^{\ell-1,k-1}\pi_\theta^{1,1}(\ell-1, k-1) + \lambda X_\theta^{\ell-1,k}\pi_\theta^{1,0}(\ell-1, k). \quad (33)$$

When $\ell = M$ and $0 < k < M$, nodes in state (θ, M, k) will switch to the states $(\theta, M, k + \delta_{\mathrm{d}})$, $\delta_{\mathrm{d}} \in \{-1, 0, 1\}$ with a probability $\pi_\theta^{0,\delta_{\mathrm{d}}}(t, M, k)$. Nodes in the states $(\theta, M - 1, k - 1)$ and $(\theta, M - 1, k)$ that have met an other node in the time interval $[t, t + \delta t]$ may reach state (θ, M, k), respectively with a probability $\pi_\theta^{1,1}(t, M - 1, k - 1)$ and $\pi_\theta^{1,0}(t, M - 1, k)$, see Figure 3. As a consequence, the evolution of $X_\theta^{M,k}(t)$ can be described by

$$\frac{dX_\theta^{M,k}}{dt} = -\lambda X_\theta^{M,k}\left(\pi_\theta^{0,1}(M, k) + \pi_\theta^{0,-1}(M, k)\right) + \lambda X_\theta^{M-1,k-1}\pi_\theta^{1,1}(M-1, k-1) + \lambda X_\theta^{M-1,k}\pi_\theta^{1,0}(M-1, k) + \lambda X_\theta^{M,k-1}\pi_\theta^{0,1}(M, k-1) + \lambda X_\theta^{M,k+1}\pi_\theta^{0,-1}(M, k+1). \quad (34)$$

Similar derivations can be made for the remaining DTN state components to obtain

$$\begin{cases} \frac{dX_\theta^{0,0}}{dt} \overset{(a)}{=} -\lambda X_\theta^{0,0}\left(\pi_\theta^{1,0}(0,0) + \pi_\theta^{1,1}(0,0)\right), \\ \frac{dX_\theta^{\ell,0}}{dt} \overset{(b)}{=} \lambda\Big(-X_\theta^{\ell,0}\left(\pi_\theta^{1,0}(\ell,0) + \pi_\theta^{1,1}(\ell,0)\right) + X_\theta^{\ell-1,0}\pi_\theta^{1,0}(\ell-1,0)\Big), \\ \frac{dX_\theta^{\ell,\ell}}{dt} \overset{(c)}{=} \lambda\Big(-X_\theta^{\ell,\ell}\left(\pi_\theta^{1,0}(\ell,\ell) + \pi_\theta^{1,1}(\ell,\ell)\right) + X_\theta^{\ell-1,\ell-1}\pi_\theta^{1,1}(\ell-1,\ell-1)\Big), \\ \frac{dX_\theta^{M,0}}{dt} \overset{(d)}{=} \lambda\Big(-X_\theta^{M,0}\pi_\theta^{0,1}(M,0) + X_\theta^{M-1,0}\pi_\theta^{1,0}(M-1,0) + X_\theta^{M,1}\pi_\theta^{0,-1}(M,1)\Big), \\ \frac{dX_\theta^{M,M}}{dt} \overset{(e)}{=} \lambda\Big(-X_\theta^{M,M}\pi_\theta^{0,-1}(M,M) + X_\theta^{M,M-1}\pi_\theta^{0,1}(M,M-1) + X_\theta^{M-1,M-1}\pi_\theta^{1,1}(M-1,M-1)\Big), \end{cases} \quad (35)$$

for any $\ell = 1 \ldots M-1$, with the initial conditions $X_\theta^{0,0}(0) = 1$ and $X_\theta^{\ell,k}(0) = 0$, $\forall \ell, k \neq 0$.

The state equation (35) is nonlinear, since each $\pi_\theta^{\delta \mathrm{m},\delta \mathrm{d}}$ depends on $X_\theta^{\ell,k}$, see (10) and (13).

6 Analysis of the DTN state equations

In what follows, the asymptotic behavior of the DTN state equations (35) is characterized. Algorithm 2 may drive $X_\theta^{\ell,k}$ to an equilibrium $\overline{X}_\theta^{\ell,k}$ at which the proportions of nodes in different states $X_\theta^{\ell,k}(t)$ do not vary any more. As a consequence, $p^{\theta 0}(t)$ defined in (10) also tends to an equilibrium $\overline{p}^{\theta 0}$.

6.1 Equilibrium of $X_\theta^{\ell,k}$

One investigates first the evolution of $X_\theta^{\ell,k}(t)$ when $\ell < M$. As shown in the following proposition, the DTN state always reaches the permanent regime.

Proposition 2. *For any $\ell < M$ and $k \leqslant \ell$, $\lim_{t\to\infty} X_\theta^{\ell,k}(t) = 0$.*

Proof: See Appendix A. □

From Proposition 2, the only possible value at equilibrium of $X_\theta^{\ell,k}(t)$ when $\ell < M$ is 0. Thus $\overline{p}^{\theta 0}$ may be written as

$$\overline{p}^{\theta 0} = \sum_{k:k/M<\nu} \overline{X}_\theta^{M,k}. \tag{36}$$

Denote $\overline{\mathbf{p}} = \left(\overline{p}^{00}, \overline{p}^{10}\right) \in \mathcal{P}_0$ with

$$\mathcal{P}_0 = \{(x,y) \in [0,1]\times[0,1] \text{ and } (x,y) \neq (0,0)\} \tag{37}$$

and consider the functions

$$h_0(\overline{\mathbf{p}}) = \frac{p_0 q_{\mathrm{FA}}(2)\,\overline{p}^{00} + p_1 q_{\mathrm{D}}(1,1)\,\overline{p}^{10}}{p_0\overline{p}^{00} + p_1\overline{p}^{10}}, \tag{38}$$

$$h_1(\overline{\mathbf{p}}) = \frac{p_0 q_{\mathrm{D}}(1,1)\,\overline{p}^{00} + p_1 q_{\mathrm{D}}(0,2)\,\overline{p}^{10}}{p_0\overline{p}^{00} + p_1\overline{p}^{10}}, \tag{39}$$

$$F_\theta(\overline{\mathbf{p}}) = \sum_{k=0}^{\lceil M\nu\rceil-1} \binom{M}{k} \left(h_\theta(\overline{\mathbf{p}})\right)^k \left(1-h_\theta(\overline{\mathbf{p}})\right)^{M-k}, \tag{40}$$

and $\mathbf{F}(\overline{\mathbf{p}}) = (F_0(\overline{\mathbf{p}}), F_1(\overline{\mathbf{p}}))$. The following proposition provides a non-linear equation that has to be satisfied by $\overline{\mathbf{p}}$. The various $\overline{X}_\theta^{M,d}$ at equilibrium are easily deduced from the solutions of the mentioned equation.

Proposition 3. *Assume that the dynamic system described by (33-35) admits some equilibrium $\overline{X}_\theta^{\ell,d}$, then $\overline{\mathbf{p}} \in \mathcal{P}_0$ is the solution of*

$$\overline{\mathbf{p}} = \mathbf{F}(\overline{\mathbf{p}}), \tag{41}$$

and for any $\theta \in \{0,1\}$ and $k \leqslant \ell$,

$$\overline{X}_\theta^{\ell,k} = \begin{cases} 0, & \forall \ell < M, \\ \binom{M}{k}\left(h_\theta(\overline{\mathbf{p}})\right)^k \left(1-h_\theta(\overline{\mathbf{p}})\right)^{M-k}, & \ell = M. \end{cases} \tag{42}$$

Proof: See Appendix B. □

6.2 Existence and unicity of the equilibrium point

Now we investigate the existence and the unicity of the solution of (41), which is rewritten in detail in (43) at the top of the next page.

For that purpose, using fixed-point theorems, one may alternatively show that for all $\mathbf{p}(0) = \left(p^{00}(0), p^{10}(0)\right) \in \mathcal{P}_0$, the discrete-time system

$$\begin{cases} p^{00}(n+1) = F_0\left(p^{00}(n), p^{10}(n)\right), \\ p^{10}(n+1) = F_1\left(p^{00}(n), p^{10}(n)\right). \end{cases} \tag{46}$$

converges to a unique equilibrium point $\left(\overline{p}^{00}, \overline{p}^{10}\right)$, which is then solution of (43).

One first shows the existence of an equilibrium using Brouwer's fixed-point theorem [28] in the following proposition.

Proposition 4. *For any $\nu \in [0,1]$,* (43) *always admits a solution, which is an equilibrium point of the dynamical system (33-35).*

Before proving Proposition 4, one first shows that $p^{00}(n)$ and $p^{10}(n)$ are contained in intervals with lower and upper bounds increasing (resp. decreasing) with n.

Lemma 5. *For any $n \in \mathbb{N}^*$ and $\theta \in \{0,1\}$, one has*

$$p_{\min}^{\theta 0}(n) \leqslant p^{\theta 0}(n) \leqslant p_{\max}^{\theta 0}(n),$$

with $p_{\min}^{\theta 0}(0) = 0$, $p_{\max}^{\theta 0}(0) = 1$, and

$$\begin{cases} p_{\min}^{\theta 0}(n+1) = F_\theta\left(p_{\min}^{00}(n), p_{\max}^{10}(n)\right), & \forall n \in \mathbb{N}^+, \\ p_{\max}^{\theta 0}(n+1) = F_\theta\left(p_{\max}^{00}(n), p_{\min}^{10}(n)\right), & \forall n \in \mathbb{N}^+. \end{cases} \tag{47}$$

Moreover,

$$p_{\min}^{00}(n+1) > p_{\min}^{00}(n), \qquad p_{\max}^{00}(n+1) < p_{\max}^{00}(n). \tag{48}$$

Proof: See Appendix C. □

Using Lemma 5, one can now prove Proposition 4.

Proof: F_0 and F_1 are both continuous functions. For some $n > 0$, consider the set $\mathcal{P}_n = \left[p_{\min}^{00}(n), p_{\max}^{00}(n)\right] \times \left[p_{\min}^{10}(n), p_{\max}^{10}(n)\right]$, where $p_{\min}^{\theta 0}(n)$ and $p_{\max}^{\theta 0}(n)$ are defined in (47). For any $\mathbf{p} = \left(p^{00}, p^{10}\right) \in \mathcal{P}_n$, one can prove using Lemma 5 that $\mathbf{F}(\mathbf{p}) \in \mathcal{P}_n$. Thus $\mathbf{F}$ maps $\mathcal{P}_n$ to $\mathcal{P}_n$. Applying Brouwer's fixed-point theorem, $\mathbf{F}$ admits a fixed point and Proposition 4 is proved. □

Sufficient conditions on p_0, p_1, q_{D}, q_{FA}, M and ν are then provided to ensure the uniqueness of this equilibrium by applying Banach's fixed-point theorem [29].

Proposition 6. *If there exists some N', such that $\forall\theta \in \{0,1\}$ and $\forall n > N'$, one has*

$$c_\theta(q_{\mathrm{FA}}(2), q_{\mathrm{D}}(0,2), q_{\mathrm{D}}(1,1), p_1, M, \nu, n) < 1, \tag{49}$$

where c_0 and c_1 are defined in (44-45), then the discrete-time system (46) *converges to a unique equilibrium point and the solution of* (43) *is unique.*

Proof: See Appendix D. □

Due to the monotonicity of $p_{\min}^{\theta 0}(n)$ and $p_{\max}^{\theta 0}(n)$ shown in Lemma 5, c_θ decreases with n. Hence, if a given ν satisfies (49) for some N', then ν will satisfy (49) for all $n \geqslant N'$ and the equilibrium is unique. If the values of p_1, q_{D}, q_{FA}, and M are fixed, then one may deduce sufficient conditions on the value of ν to have a unique equilibrium point. See Example 7.

$$\begin{cases} \overline{p}^{00} = F_0\left(\overline{p}^{00},\overline{p}^{10}\right) = \sum_{k:k/M<\nu}\binom{M}{k}\left(\frac{p_0 q_{\mathrm{FA}}(2)\overline{p}^{00}+p_1 q_{\mathrm{D}}(1,1)\overline{p}^{10}}{p_0\overline{p}^{00}+p_1\overline{p}^{10}}\right)^k\left(\frac{p_0(1-q_{\mathrm{FA}}(2))\overline{p}^{00}+p_1(1-q_{\mathrm{D}}(1,1))\overline{p}^{10}}{p_0\overline{p}^{00}+p_1\overline{p}^{10}}\right)^{M-k}, \\ \overline{p}^{10} = F_1\left(\overline{p}^{00},\overline{p}^{10}\right) = \sum_{k:k/M<\nu}\binom{M}{k}\left(\frac{p_0 q_{\mathrm{D}}(1,1)\overline{p}^{00}+p_1 q_{\mathrm{D}}(0,2)\overline{p}^{10}}{p_0\overline{p}^{00}+p_1\overline{p}^{10}}\right)^k\left(\frac{p_0(1-q_{\mathrm{D}}(1,1))\overline{p}^{00}+p_1(1-q_{\mathrm{D}}(0,2))\overline{p}^{10}}{p_0\overline{p}^{00}+p_1\overline{p}^{10}}\right)^{M-k}. \end{cases} \tag{43}$$

$$c_0(q_{\mathrm{FA}}(2),q_{\mathrm{D}}(0,2),q_{\mathrm{D}}(1,1),p_1,M,\nu,n) = \frac{M\left(q_{\mathrm{D}}(1,1)-q_{\mathrm{FA}}(2)\right)p_0 p_1 p_{\max}^{00}(n)\,p_{\max}^{10}(n)}{(p_0 p_{\min}^{00}(n)+p_1 p_{\min}^{10}(n))((1-q_{\mathrm{FA}}(2))p_0 p_{\min}^{00}(n)+(1-q_{\mathrm{D}}(1,1))p_1 p_{\min}^{10}(n))}, \tag{44}$$

$$c_1(q_{\mathrm{FA}}(2),q_{\mathrm{D}}(0,2),q_{\mathrm{D}}(1,1),p_1,M,\nu,n) = \frac{M\left(q_{\mathrm{D}}(0,2)-q_{\mathrm{D}}(1,1)\right)p_0 p_1 p_{\max}^{00}(n)\,p_{\max}^{10}(n)}{(p_0 p_{\min}^{00}(n)+p_1 p_{\min}^{10}(n))((1-q_{\mathrm{D}}(1,1))p_0 p_{\min}^{00}(n)+(1-q_{\mathrm{D}}(0,2))p_1 p_{\min}^{10}(n))}, \tag{45}$$

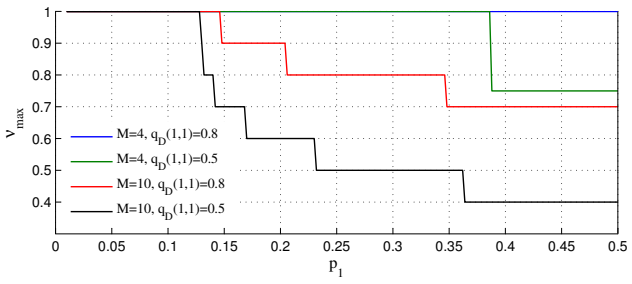

Fig. 4. Upper bounds of ν to satisfy (49), with $q_{\mathrm{FA}}(2)=0.05$, $q_{\mathrm{D}}(0,2)=0.9$, $q_{\mathrm{D}}(1,1)\in\{0.5,0.8\}$, $M\in\{4,10\}$, and $p_1\in[0.05,0.5]$.

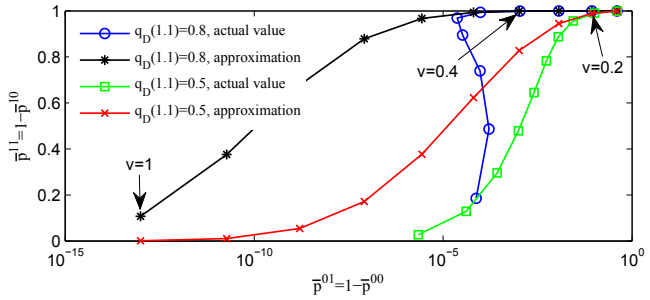

Fig. 5. Approximate p^{11} as a function of approximate p^{01}, for various ν and fixed $M=10$.

Example 7. Consider $q_{\mathrm{FA}}(2)=0.05$, $q_{\mathrm{D}}(0,2)=0.9$, $q_{\mathrm{D}}(1,1)\in\{0.5,0.8\}$, $M\in\{4,10\}$, and $p_1\in[0.05,0.5]$. One verifies whether (49) is satisfied considering $n=10$ for different values of ν. One obtains that (49) holds if $0<\nu\leqslant\nu_{\max}$, where $\nu_{\max}$ depends on the values of p_1, q_{D}, q_{FA}, and M. See Figure 4 for the numerical values of $\nu_{\max}$ in each case.

6.3 Equilibrium point as $M\to\infty$

Both $\overline{p}^{00}$ and $\overline{p}^{10}$ can be seen as functions of M. As $M\to\infty$, Algorithm 2 turns into Algorithm 1. In this situation, if ν is properly chosen, the probabilities of false alarm and non-detection tend to zero, as shown in Proposition 8.

Proposition 8. *If* $q_{\mathrm{FA}}(2)<\nu<q_{\mathrm{D}}(1,1)$, *then* (43) *has a unique solution and*

$$\lim_{M\to\infty}\overline{p}^{00}=1, \qquad \lim_{M\to\infty}\overline{p}^{10}=0. \tag{50}$$

Proof: See Appendix E. □

7 Approximations of the Equilibrium

Closed-form expressions for $\overline{p}^{00}$ and $\overline{p}^{10}$ are difficult to obtain from (43). This section introduces an approximation of (43) from which some insights may be obtained on the way ν should be chosen.

Since $\overline{p}^{10}$ represents the proportion of nodes with defective sensors that have not detected their status, the value of $\overline{p}^{10}$ should be small. From (38-39) one sees that $\lim_{\overline{p}^{10}\to 0}h_0=q_{\mathrm{FA}}(2)$ and $\lim_{\overline{p}^{10}\to 0}h_1=q_{\mathrm{D}}(1,1)$, thus one may consider the following approximations

$$h_0\approx\widetilde{h}_0=q_{\mathrm{FA}}(2), \quad h_1\approx\widetilde{h}_1=q_{\mathrm{D}}(1,1). \tag{51}$$

Therefore, (43) may be rewritten as

$$\begin{cases} \widetilde{p}^{00} = \sum_{k:k/M<\nu}\binom{M}{k}\left(q_{\mathrm{FA}}(2)\right)^k\left(1-q_{\mathrm{FA}}(2)\right)^{M-k}, \\ \widetilde{p}^{10} = \sum_{k:k/M<\nu}\binom{M}{k}\left(q_{\mathrm{D}}(1,1)\right)^k\left(1-q_{\mathrm{D}}(1,1)\right)^{M-k}. \end{cases} \tag{52}$$

from which one deduces approximate values $\widetilde{X}_0^{M,k}$ of $X_0^{M,k}$ at equilibrium

$$\begin{cases} \widetilde{X}_0^{M,k} = \binom{M}{k}\left(q_{\mathrm{FA}}(2)\right)^k\left(1-q_{\mathrm{FA}}(2)\right)^{M-k}, \\ \widetilde{X}_1^{M,k} = \binom{M}{k}\left(q_{\mathrm{D}}(1,1)\right)^k\left(1-q_{\mathrm{D}}(1,1)\right)^{M-k}. \end{cases} \tag{53}$$

For any fixed value of M, $q_{\mathrm{FA}}(2)$, and $q_{\mathrm{D}}(1,1)$, the values of *detection rate* ($\overline{p}^{11}$) and *false alarm rate* ($\overline{p}^{01}$) at equilibrium can be predicted using (52), since $\overline{p}^{01}=1-\overline{p}^{00}$ and $\overline{p}^{11}=1-\overline{p}^{10}$. Consider for example $M=10$, $q_{\mathrm{FA}}(2)=0.05$, and $q_{\mathrm{D}}(1,1)=0.8$. Figure 5 presents $\widetilde{p}^{11}$ as a function of $\widetilde{p}^{01}$ for different values of ν. This figure is helpful to choose the value of ν to meet different performance requirements. The actual values of $\overline{p}^{11}$ and $\overline{p}^{01}$ are also shown in Figure 5, which are very close to $\widetilde{p}^{11}$ and $\widetilde{p}^{01}$, in the region where $\overline{p}^{11}$ is close to 1.

8 Numerical Results

8.1 Numerical verification of theoretical results

This section presents first the solution of the state equation (35) describing the evolution of the proportion of nodes in various states. Algorithm 2 is simulated considering a random displacement of nodes without constraint on their speed. This allows to verify the correctness of the theoretical results presented in this paper.

Consider a LODT where $q_{\mathrm{FA}}(0,2)=0.05$, $q_{\mathrm{D}}(1,1)=0.8$, and $q_{\mathrm{D}}(0,2)=0.9$. Besides, $p_0=0.9$, $p_1=0.1$, $M=4$, $\nu=0.4$, and $\lambda=1$. Figure 6 presents the evolution of the proportion of nodes with good sensors (top part) and defective sensors (bottom part) in different states, obtained by solving (35). Note that Δt represents the duration of a unit time slot used in the simulation. One observes that the proportion of nodes in each state becomes almost constant as $t/\Delta t\geqslant 15$. For the nodes with $\theta=0$, only two states are such that $X_0^{\ell,k}>0.05$, $(0,4,0)$ and $(0,4,1)$, while the others

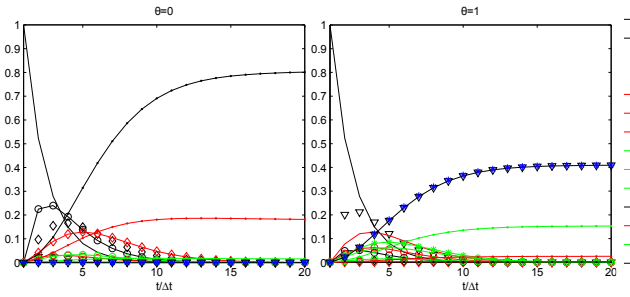

Fig. 6. Evolution of $X_0^{\ell,k}(t)$ (left) and $X_1^{\ell,k}(t)$ (right) obtained from (35), in the case where $q_{\text{FA}}(0,2) = 0.05$, $q_{\text{D}}(1,1) = 0.8$, $q_{\text{D}}(0,2) = 0.9$, $M = 4$, $\nu = 0.4$, and $\lambda = 1$.

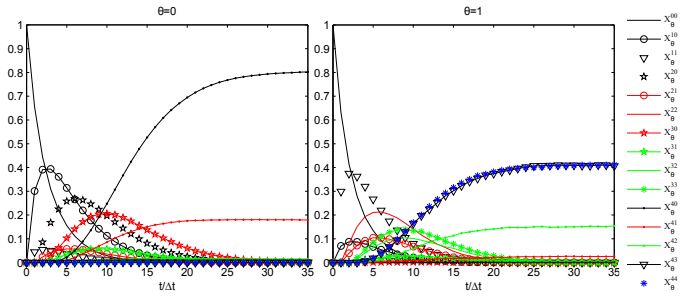

Fig. 7. Evolution of $X_0^{\ell,k}(t)$ (left) and $X_1^{\ell,k}(t)$ (right) by simulations with the jump model, in the case where $q_{\text{FA}}(0,2) = 0.05$, $q_{\text{D}}(1,1) = 0.8$, $q_{\text{D}}(0,2) = 0.9$, $M = 4$, $\nu = 0.4$, and $\lambda\Delta t = 0.33$.

are very close to 0. For the nodes with $\theta = 1$, only $X_1^{4,4}$, $X_1^{4,3}$, and $X_1^{4,2}$ are relatively large. Since there is no common (ℓ, k) such that both $X_0^{\ell,k}$ and $X_1^{\ell,k}$ have unnegligeable values, the accuracy of the algorithm can be very good. With $\nu = 0.4$, one has $\overline{p}^{00} = 0.985$ and $\overline{p}^{10} = 0.027$. Only 1.5% of the good nodes believe they are carrying defective sensors. Less than 3% of the nodes with defective sensors have not been detected.

Consider now a set $\mathcal{S}$ of $N_S = 1000$ moving nodes uniformly distributed over a square of unit area. In the first displacement model (jump motion model): Node i randomly chooses its location at time instant $(k+1)\Delta t$, independently from its previous location at time $k\Delta t$. Two nodes communicate only at discrete time instants $k\Delta t$ when their distance is less than r_0. Node i has its neighbors in the set $\mathcal{N}_i = \{j \in \mathcal{S} : 0 < R_{i,j} \leq r_0\}$, where $R_{i,j}$ is the distance between Nodes i and j. Furthermore, if $|\mathcal{N}_i| > 1$, we assume that Node i communicates only with its closest neighbor. Denote $\rho = \pi r_0^2 N_S$ as the average value of $|\mathcal{N}_i|$. The cardinality of $\mathcal{N}_i$ approximately follows a Poisson distribution as N_S is large enough, the inter-contact probability is thus

$$\lambda\Delta t = \mathbb{P}\{|\mathcal{N}_i| = 1\} = \rho \exp(-\rho).$$

In the Monte-Carlo simulations, we set $r_0 = 0.014$, so that $\rho \approx 0.6$ and $\lambda\Delta t \approx 0.33$. Using the same values of M, ν, q_{D}, and q_{FA} as in Figure 6, the simulation results for this jump motion model are shown in Figure 7. Comparing Figure 6 and Figure 7, one remarks that the state evolution in the transient phase has similar shape but with different convergence speed, which depends mainly on λ. Figure 8 shows a good match between theory and simulation for the proportions of states at equilibrium. The approximation of $\overline{X}_\theta^{4,k}$ using (53) is also presented in Figure 8, which is very close to its actual value.

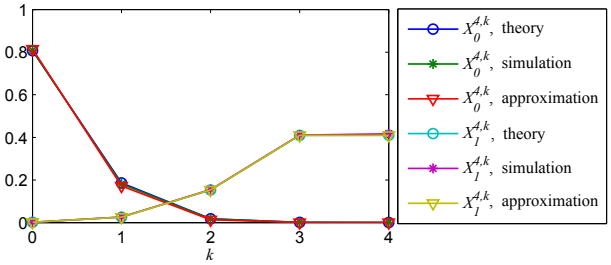

Fig. 8. Comparison of $\overline{X}_\theta^{4,k}$ at the equilibrium.

8.2 Simulation with Brownian motion model

Consider now a Brownian motion model where each node is moving with a random speed. Each node changes its orientation when it reaches the boundary of the unit square. Define $\boldsymbol{O}_i = (o_x^i, o_y^i)$ as the location of Node i. Consider a second order mobility model, *i.e.*, $d^2 o_x/dt^2 = v_x$ and $d^2 o_y/dt^2 = v_y$, where $v_x, v_y \sim \mathcal{N}\left(0, (\sigma r_0)^2\right)$.

Consider $\sigma \in \{0.1, 1\}$, $q_{\text{FA}}(2) = 0.05$, $q_{\text{D}}(1,1) = 0.8$, $q_{\text{D}}(0,2) = 0.9$, $M = 10$, and $\nu = 0.4$. Figure 9 compares the evolution of p^{01} and p^{10} as functions of time for the jump motion model and the Brownian motion model, with fixed $\rho \approx 0.6$. At equilibrium, the performance obtained for both models is quite close. However, the convergence speed depends on the inter-contact rate λ. When $\sigma = 0.1$, the algorithm converges slowly in the Brownian motion model. When $\sigma = 1$, which results to a larger value of λ, the evolution of p^{01} and p^{10} with the Brownian motion model are close to the jump motion model.

At the beginning of the algorithm, each node believes that its sensors are good, thus $p^{01}(0) = 0$ and $p^{10}(0) = 1$. During the algorithm, $p^{10}(t)$ decreases in the transient phase until it reaches the equilibrium. Whereas, $p^{01}(t)$ increases at first and then decreases to the equilibrium. This comes from the fact that $p^{10}(t)$ is large at the beginning and the LODT performed on a good node often detects outliers.

8.3 Simulation with real databases

In this section, Algorithm 2 is executed on some experimental databases instead of motion models. These databases, provided by the MIT Reality Mining Project [30] and the

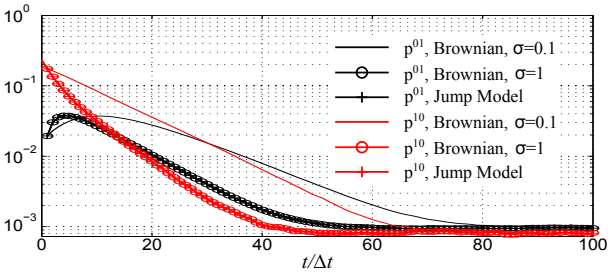

Fig. 9. Evolution of p^{01} and p^{10} for the two moving models, with $\sigma \in \{0.1, 1\}$, $q_{\text{FA}}(2) = 0.05$, $q_{\text{D}}(1,1) = 0.8$, $q_{\text{D}}(0,2) = 0.9$, $M = 10$ and $\nu = 0.4$.

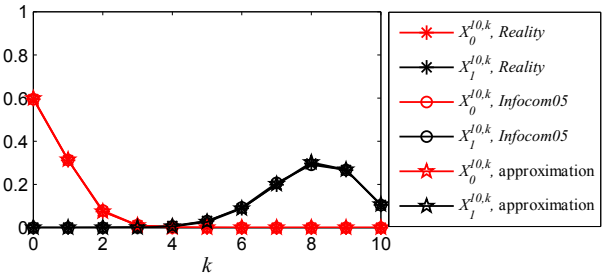

Fig. 11. Comparison of $\overline{X}_\theta^{10,k}$ at the equilibrium obtained using the *Reality* database, the *Infocom05* database, and predicted by the approximation (53).

Haggle Project [31], are well investigated in several previous works, *e.g.*, [3]. In this work, we use the following databases:

- *Reality*, where $N_S = 97$, lasts more than 200 days with about 111 inter-contacts per day.
- *Infocom05*, where $N_S = 41$, lasts 3 days with approximately 312 inter-contacts every hour.

More specifically, one is interested in the inter-contact trace, *i.e.*, which pair of nodes have a meeting at which time. The traces were taken from [32], which are converted from the original databases [30], [31].

Consider again the following parameters: $q_{\text{FA}}(2) = 0.05$, $q_{\text{D}}(1,1) = 0.8$, $q_{\text{D}}(0,2) = 0.9$, $M = 10$, and $\nu = 0.4$. Monte-Carlo simulations are performed 500 times for each database. In each test, N_D nodes with random index are chosen to be defective. One sets $N_D = 10$ in *Infocom05* and $N_D = 20$ in *Reality*. At the top of Figure 10, the index of the active nodes (which have contact with the others) are presented at each time to show the frequence of the inter-contacts at different epochs. The evolution of p^{10} and p^{01} is plotted at the bottom of Figure 10. Interestingly, both p^{10} and p^{01}, obtained by all the three databases, decrease to 10^{-3} after a sufficient long time. One also observes that the convergence speed of p^{10} and p^{01} is highly related to the inter-contact rate (reflected by the density of points in the sub-figures at the top): variations are significant at beginning of working hours.

Figure 11 represents the states at equilibrium $\overline{X}_\theta^{M,k}$ obtained by using the databases *Reality* and *Infocom05*, and also by the approximation (53). There is an excellent match between the values at equilibrium predicted by theory and those obtained in practice.

8.4 Influence of the parameters

This section characterizes the influence of the parameters, such as p_1, $q_D(1,1)$, and M, on the performance of Algorithm 2. The jump motion model is used throughout this section to describe the displacement of the nodes.

Consider fixed $q_{\text{FA}}(2) = 0.05$, $q_{\text{D}}(1,1) = 0.8$, $q_{\text{D}}(0,2) = 0.9$, the evolution of p^{10} and p^{01} for various $p_1 \in \{0.1, 0.5\}$ and $M \in \{4, 10, 20\}$ is shown in Figure 12. For each different case, the value of ν is chosen such that it minimises $\widetilde{p}^{01} + \widetilde{p}^{10}$. One observes that a large M leads to a better performance at equilibrium. The price to be paid is a longer time required to reach equilibrium. When $M = 10$, both $\overline{p}^{10}$ and $\overline{p}^{01}$ are around 10^{-3}. The proportion of the nodes with defective sensors has also an impact on the convergence speed of the algorithm. For example, when p_1 is large, more time is needed to achieve a given level of performance (in terms of $\overline{p}^{10}$ and $\overline{p}^{01}$).

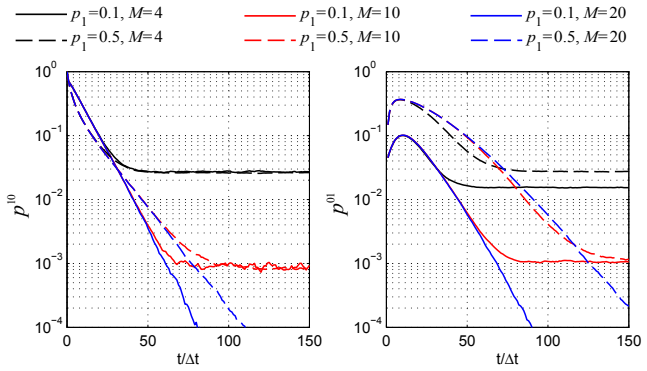

Fig. 12. Evolution of p^{10} and p^{01} for various $M \in \{4, 10, 20\}$ and $p_1 \in \{0.1, 0.5\}$, with $q_{\text{FA}}(2) = 0.05$, $q_{\text{D}}(1,1) = 0.8$, $q_{\text{D}}(0,2) = 0.9$.

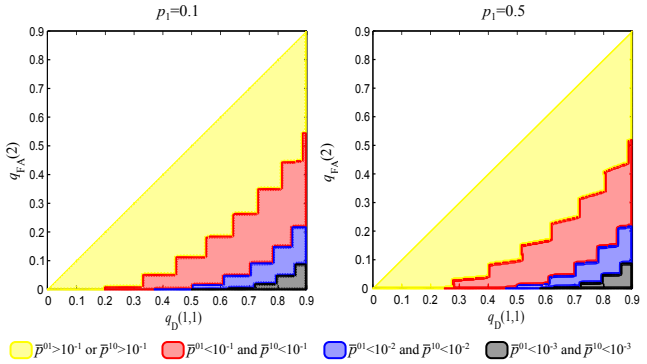

Fig. 13. Achievable $\overline{p}^{10}$ or $\overline{p}^{01}$ for different values of the pair $(q_{\text{D}}(1,1), q_{\text{FA}}(2))$ when $p_1 = 0.1$ (left) and for $p_1 = 0.5$ (right).

To show the effectiveness of the proposed DFD algorithm, consider now $q_{\text{D}}(0,2) = 0.9$ and $M = 10$. For $p_1 = 0.1$ and $p_1 = 0.5$, one is interested in the achievable $\overline{p}^{10}$ and $\overline{p}^{01}$ for $0 \leqslant q_{\text{FA}}(2) < q_{\text{D}}(0,2)$ and $q_{\text{FA}}(2) < q_{\text{D}}(1,1) \leqslant q_{\text{D}}(0,2)$. Four areas are considered:

- Area 3: both $\overline{p}^{10}$ and $\overline{p}^{01}$ are less than 10^{-3} ;
- Area 2: both $\overline{p}^{10}$ and $\overline{p}^{01}$ are less than 10^{-2} ;
- Area 1: both $\overline{p}^{10}$ and $\overline{p}^{01}$ are less than 10^{-1};
- Area 0: either $\overline{p}^{10}$ or $\overline{p}^{01}$ cannot be less than 10^{-1}.

Figure 13 shows partition of the $(q_{\text{D}}(1,1), q_{\text{FA}}(2))$ triangle in four areas, represented in different colors. The ratio of defective nodes in the network has not a significant impact on the performance at the equilibrium, even when 50% of nodes are defective.

9 Conclusion

This paper presents a fully distributed algorithm allowing each node of a DTN to estimate the status of its own sensors using LODT performed during the meeting of nodes. The DFD algorithm is analyzed considering a Markov model of the evolution of the proportion of nodes with a given belief in their status. This model is then used to derive

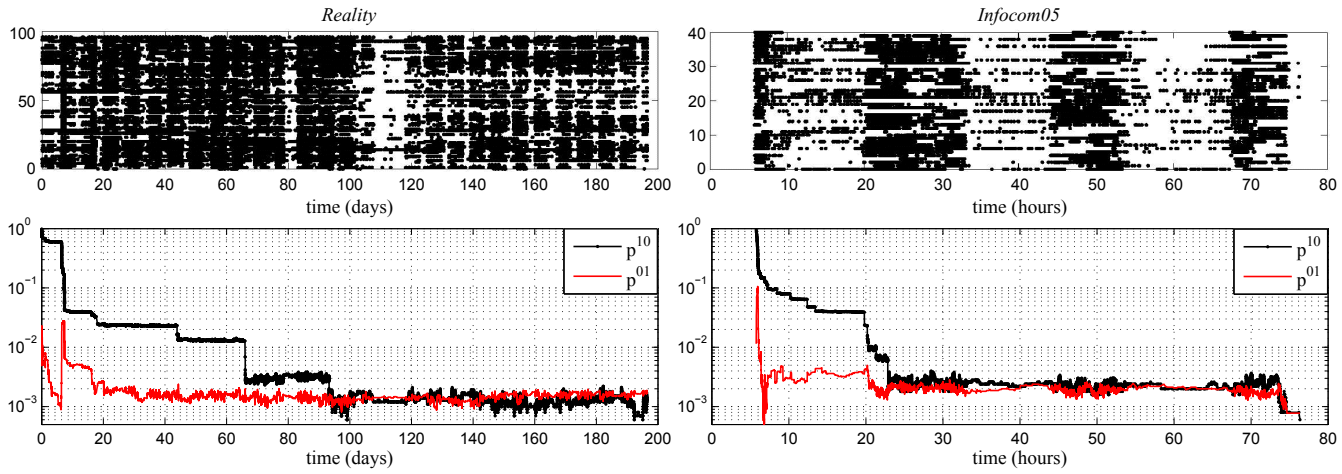

Fig. 10. Indexes of active nodes (having met another node) at different time (top) and evolution of p^{01} and p^{10} (bottom) obtained by using the *Reality* database (left) and the *Infocom05* database (right), with $q_{\mathsf{FA}}(2) = 0.05$, $q_{\mathsf{D}}(1,1) = 0.8$, $q_{\mathsf{D}}(0,2) = 0.9$, $M = 10$, and $\nu = 0.4$.

the evolution of the proportions of the nodes in different states. The existence and uniqueness of an equilibrium is discussed. Interestingly, the proportions at the equilibrium follow a Binomial distribution. Approximations of these proportions of nodes provide a clear guide to properly choose the decision parameter of the DFD algorithm. In the simulations, a jump motion model and a Brownian motion model are considered. The results show a good match with theory. The convergence speed of the DFD algorithm depends on the inter-contact rate and on the proportion of nodes with defective sensors p_1. Nevertheless, p_1 has not a significant impact on the non-detection and false alarm rates at equilibrium, showing the robustness of the approach to a large number of defective nodes.

Further research will be dedicated to an adaptation of ν with time to increase the convergence speed of the proposed DFD algorithm. This may be particularly important in variants of the considered problem, such as malware detection.

Appendix A
Proof of Proposition 2

For the proof, one considers first the following lemmas.

Lemma 9. *If*

$$\lim_{t\to\infty} \int_0^t \left(p_0 p^{00}(\tau) + p_1 p^{10}(\tau)\right) d\tau = \infty \tag{54}$$

then $p_0 p^{00}(t) + p_1 p^{10}(t) > 0$ *for all* $t \in \mathbb{R}^+$.

Proof: Since $p_0 > 0$, $p_1 > 0$, $p^{00} \geqslant 0$, and $p^{10} \geqslant 0$, it suffices to prove that

$$p^{00}(t) + p^{10}(t) \neq 0 \qquad \forall t > 0. \tag{55}$$

Assume that there exists a time instant $t^* > 0$, such that $p^{00}(t^*) + p^{10}(t^*) = 0$. As a consequence, at time t^*, all nodes in the network believe themselves as carrying defective sensors. As a consequence, no node will transmit its data to its neighbors. No LODTs will be performed after time t^* and the state of nodes will remain constant. Hence, if $p^{00}(t^*) + p^{10}(t^*) = 0$ for some t^*, then $p^{00}(t) + p^{10}(t) = 0$ for all $t > t^*$. Consequently,

$$\lim_{t\to\infty} \int_0^t \left(p_0 p^{00}(\tau) + p_1 p^{10}(\tau)\right) d\tau = \int_0^{t^*} \left(p_0 p^{00}(\tau) + p_1 p^{10}(\tau)\right) d\tau,$$

which contradicts (54). □

Lemma 10. *The property* (54) *is always satisfied.*

Proof: From (35-a), one has

$$X_\theta^{0,0}(t) = \exp\left(-\lambda \int_0^t \left(p_0 p^{00}(\tau) + p_1 p^{10}(\tau)\right) d\tau\right). \tag{56}$$

Assume that there exists $C^* > 0$ such that

$$\lim_{t\to\infty} \int_0^t \left(p_0 p^{00}(\tau) + p_1 p^{10}(\tau)\right) d\tau \leqslant C^* \tag{57}$$

then $\forall t \geqslant 0$, one has

$$\int_0^t \left(p_0 p^{00}(\tau) + p_1 p^{10}(\tau)\right) d\tau \leqslant C^*. \tag{58}$$

Combining (56) and (58), one gets

$$X_\theta^{0,0}(t) \geqslant \exp(-\lambda C^*) > 0. \tag{59}$$

Moreover, from (10), one has $p^{00}(\tau) \geqslant X_\theta^{0,0}(\tau)$, leading to

$$\int_0^t \left(p_0 p^{00}(\tau) + p_1 p^{10}(\tau)\right) d\tau \geqslant \int_0^t p_0 X_\theta^{0,0}(\tau) d\tau > p_0 \exp(-\lambda C^*)\, t. \tag{60}$$

Since $\exp(-\lambda C^*)\, t \to \infty$ as $t \to \infty$, (60) leads to a violation of the hypothesis (57). Hence, one always has (54). □

The proof of Proposition 2 is then by induction. Starting with (35-a), one has (56). Since (54) is satisfied according to Lemma 10, for any $\xi > 0$, there exists $t_{00} > 0$ such that $t > t_{00}$ implies $X_\theta^{0,0}(t) < \xi$ and $\lim_{t\to\infty} X_\theta^{0,0}(t) = 0$.

Then, assume that for any $\ell \leqslant M-1$, and $\xi > 0$, there exists $t_{(\ell-1)0} > \cdots > t_{00}$ such that $t > t_{(\ell-1)0}$ implies $X_\theta^{j,0}(t) < \xi$ for $j = 0, \ldots, \ell-1$. One has to show now that there exists $t_{\ell 0} > t_{(\ell-1)0}$ such that $X_\theta^{\ell,0}(t) < \xi$ for all $t > t_{\ell 0}$.

Define $Z_\theta^{\ell,0}(t) = \sum_{j=0}^{\ell} X_\theta^{j,0}(t)$. From (35$a$) and (35$b$), one has

$$\frac{dZ_\theta^{\ell,0}}{dt} = -\lambda\left(v(t)\, Z_\theta^{\ell-1,0}(t) + \left(p_0 p^{00}(t) + p_1 p^{10}(t)\right) X_\theta^{\ell,0}(t)\right),$$

where $v(t) = \pi_\theta^{1,1}(t,\ell,k)$, since $\pi_\theta^{1,0}$ and $\pi_\theta^{1,1}$ do not depend on ℓ and k when $\ell < M$. Using (55) one has $dZ_\theta^{\ell,0}/dt < 0$ for any $X_\theta^{\ell 0} > 0$. As a consequence, $Z_\theta^{\ell,0}(t)$ decreases until

$X_\theta^{\ell,0}(t)$ reaches 0. Hence, for any $\xi > 0$, there exists $t_{\ell,0} > t_{(\ell-1)0}$, such that $X_\theta^{\ell,0} < \xi$ and $\lim_{t\to\infty} X_\theta^{\ell,0}(t) = 0$.

In the same way, using (35c) and the previous results that $X_\theta^{\ell k}(t) \to 0$ with $k = 1,\dots,M-2$ and $\ell = k,\dots,M-2$, one can prove that for any $k = 1,\dots,M-1$, $X_\theta^{\ell',(k+1)}(t)$ tends to zero as $t \to \infty$, with any $\ell' = k+1,\dots,M-1$.

Appendix B
Proof of Proposition 3

According to Proposition 2, one has $\overline{X}_\theta^{\ell,k} = 0$, for all $\ell < M$ and $k \leqslant \ell$. To evaluate $\overline{X}_\theta^{M,k}$, one thus considers the following simplified dynamics derived from (35) for $\theta \in \{0,1\}$,

$$\begin{cases} \frac{dX_\theta^{M,0}}{dt} = \lambda\Big(-X_\theta^{M,0}\pi_\theta^{0,1}(M,0) + X_\theta^{M,1}\pi_\theta^{0,-1}(M,1)\Big), \\ \frac{dX_\theta^{M,M}}{dt} = \lambda\Big(-X_\theta^{M,M}\pi_\theta^{0,-1}(M,M) + X_\theta^{M,M-1}\pi_\theta^{0,1}(M,M-1)\Big), \\ \frac{dX_\theta^{M,k}}{dt} = \lambda\Big(-X_\theta^{M,k}\left(\pi_\theta^{0,-1}(M,k) + \pi_\theta^{0,1}(M,k)\right) \\ \qquad + X_\theta^{M,k+1}\pi_\theta^{0,-1}(M,k+1) + X_\theta^{M,k-1}\pi_\theta^{0,1}(M,k-1)\Big). \end{cases} \tag{61}$$

At equilibrium, one has $dX_\theta^{M,k}(t)/dt = 0$ for all $k \leqslant M$. Moreover, the transition probabilities do not vary any more. Let $\overline{\boldsymbol{X}}_\theta^M = \left(\overline{X}_\theta^{M,1},\dots,\overline{X}_\theta^{M,M}\right)^{\mathrm{T}}$, $a_\theta(k) = \pi_\theta^{0,1}(M,k)$, and $b_\theta(k) = \pi_\theta^{0,-1}(M,k)$. From (61), one deduces that the vector $\overline{\boldsymbol{X}}_\theta^M$ should satisfy $\boldsymbol{\Psi}_\theta \cdot \overline{\boldsymbol{X}}_\theta^M = \mathbf{0}$ where

$$\boldsymbol{\Psi}_\theta = \begin{pmatrix} -a_\theta(0) & b_\theta(1) & & \\ a_\theta(0) & -a_\theta(1) - b_\theta(1) & b_\theta(2) & \\ & \ddots & \ddots & \ddots \\ & & a_\theta(M-1) & -b_\theta(M) \end{pmatrix}.$$

Summing Lines 1 to $k+1$, for all $k = 0,\dots,M-1$, one obtains $a_\theta(k)\,\overline{X}_\theta^{M,k} = b_\theta(k+1)\,\overline{X}_\theta^{M,k+1}$, which leads to

$$\overline{X}_\theta^{M,k} = \overline{X}_\theta^{M,0}\prod_{j=0}^{k-1}\frac{a_0(j)}{b_0(j+1)}. \tag{62}$$

One evaluates

$$\frac{a_\theta(j)}{b_\theta(j+1)} = \frac{\pi_\theta^{0,1}(M,j)}{\pi_\theta^{0,-1}(M,j+1)} = \eta_\theta\frac{M-j}{j+1}, \tag{63}$$

where using (29) and (30), one has

$$\begin{cases} \eta_0 = \frac{p_0 q_{\mathrm{FA}}(2)\overline{p}^{00} + p_1 q_{\mathrm{D}}(1,1)\overline{p}^{10}}{p_0(1-q_{\mathrm{FA}}(2))\overline{p}^{00} + p_1(1-q_{\mathrm{D}}(1,1))\overline{p}^{10}}, \\ \eta_1 = \frac{p_0 q_{\mathrm{D}}(1,1)\overline{p}^{00} + p_1 q_{\mathrm{D}}(0,2)\overline{p}^{10}}{p_0(1-q_{\mathrm{D}}(1,1))\overline{p}^{00} + p_1(1-q_{\mathrm{D}}(0,2))\overline{p}^{10}}. \end{cases} \tag{64}$$

with $\overline{p}^{00}$ and $\overline{p}^{10}$ defined in (36).

From (62) and (63), one deduces

$$\begin{aligned} \overline{X}_\theta^{M,k} &= \overline{X}_\theta^{M,0}\prod_{j=0}^{k-1}\left(\eta_\theta\frac{M-j}{j+1}\right) \\ &= \overline{X}_\theta^{M,0}\eta_\theta^k\frac{M\cdot(M-1)\cdot(M-k+1)}{1\cdot 2\cdot\cdots\cdot k} = \binom{M}{k}\eta_\theta^k\overline{X}_\theta^{M,0}. \end{aligned} \tag{65}$$

Since $\sum_{k=0}^M \overline{X}_\theta^{M,k} = 1$, one has

$$1 = \sum_{k=0}^M\binom{M}{k}\eta_\theta^k\overline{X}_\theta^{M,0} = (\eta_\theta+1)^M\,\overline{X}_\theta^{M,0}. \tag{66}$$

From (65) and (66), $\forall k = 0,\dots,M$,

$$\overline{X}_\theta^{M,k} = \binom{M}{k}\left(\frac{\eta_\theta}{\eta_\theta+1}\right)^k\left(\frac{1}{\eta_\theta+1}\right)^{M-k} = \binom{M}{k}(h_\theta)^k(1-h_\theta)^{M-k} \tag{67}$$

with $h_\theta = \frac{\eta_\theta}{\eta_\theta+1}$. Introducing (67) into (36), one obtains (41) with F_θ defined in (40). Thus one needs to solve (41) to determine $\overline{\mathbf{p}}$, which is then used to deduce $\overline{X}_\theta^{M,d}$ using (67).

Appendix C
Proof of Lemma 5

To prove Lemma 5, one needs first investigate the monotonicity of F_θ. To lighten the notations, let $\alpha = q_{\mathrm{FA}}(2)$, $\beta = q_{\mathrm{D}}(1,1)$ and $\gamma = q_{\mathrm{D}}(0,2)$. Then h_0 and h_1 defined in (38-39) can be rewritten as

$$h_0(x,y) = \frac{\alpha p_0 x + \beta p_1 y}{p_0 x + p_1 y},\ h_1(x,y) = \frac{\beta p_0 x + \gamma p_1 y}{p_0 x + p_1 y}, \tag{68}$$

with $(x,y) \in \mathcal{P}_0$. One starts showing some monotonicity properties.

Lemma 11. *If $\alpha < \beta < \gamma$, then h_0 and h_1 are decreasing with x and increasing with y, for all $(x,y) \in \mathcal{P}_0$. If $\beta = \gamma$, then $h_1 = \beta = \gamma$ is a constant.*

Proof: Since $\alpha < \beta \leqslant \gamma$, one has

$$\begin{aligned} \frac{\partial h_0}{\partial x} &= \frac{(\alpha-\beta)\,p_0p_1y}{(p_0x+p_1y)^2} \leqslant 0, \quad \frac{\partial h_0}{\partial y} = \frac{(\beta-\alpha)\,p_0p_1x}{(p_0x+p_1y)^2} \geqslant 0, \\ \frac{\partial h_1}{\partial x} &= \frac{(\beta-\gamma)\,p_0p_1y}{(p_0x+p_1y)^2} \leqslant 0, \quad \frac{\partial h_1}{\partial y} = \frac{(\gamma-\beta)\,p_0p_1x}{(p_0x+p_1y)^2} \geqslant 0. \end{aligned}$$

then Lemma 11 can be proved. □

Lemma 12. *For $z \in [0,1]$, the family of functions*

$$f_i(z) = z^i(1-z)^{M-i},\ i = 0,1\dots,M. \tag{69}$$

are increasing over $[0, \frac{i}{M}]$ and decreasing over $[\frac{i}{M}, 1]$.

Proof: Consider three possible situations: 1) If $i = 0$, $f_0(z) = (1-z)^M$ is decreasing over $[0,1]$. 2) If $i = M$, $f_M(z) = z^M$ is increasing over $[0,1]$. 3) If $1 \leqslant i \leqslant M-1$,

$$\frac{df_i}{dz} = z^{i-1}(1-z)^{M-i-1}(i-Mz), \tag{70}$$

and $df_i/dz \geqslant 0$ when $z \in [0, \frac{i}{M}]$ and $df_i/dz \leqslant 0$ when $z \in [\frac{i}{M}, 1]$. Therefore, Lemma 12 holds $\forall i = 0,\dots,M$. □

Lemma 13. *If $0 < \nu < 1$, the function*

$$g(z) = \sum_{i:i/M<\nu}\binom{M}{i}f_i(z) = \sum_{i:i/M<\nu}\binom{M}{i}z^i(1-z)^{M-i}, \tag{71}$$

is decreasing for all $z \in [0,1]$.

Proof: First, consider $z \in [\nu, 1]$. In (71), each i in the sum is such that $\frac{i}{M} < \nu \leqslant z$. From Lemma 12, $f_i(z)$ is a decreasing function for any $\frac{i}{M} < z$, thus $g(z)$ is also decreasing with z.

Now, consider $z \in [0,\nu]$, one rewrites (71) as

$$g(z) = 1 - \sum_{i:i/M\geqslant\nu}\binom{M}{i}f_i(z), \tag{72}$$

in which each i in the sum is such that $z < \nu \leqslant \frac{i}{M}$. Applying again Lemma 12, since $f_i(z)$ is an increasing function for

any $z \leqslant \frac{i}{M}$, the sum in (72) is also increasing with z and $g(z)$ is decreasing. Thus $g(z)$ is a decreasing function of z over $[0,1]$. □

Considering the functions h_θ and g, then one may rewrite F_θ as $F_\theta(x,y) = g(h_\theta(x,y))$, $\forall\theta \in \{0,1\}$. The monotonicity of F_0 and F_1 is shown in the following lemma.

Lemma 14. *If $\alpha < \beta < \gamma$, then F_0 and F_1 are increasing functions of x and decreasing functions of y, for all $(x,y) \in \mathcal{P}_0$. If $\beta = \gamma$, then $F_1 = g(\beta) = g(\gamma)$ is a constant.*

Proof: The proof of obtained by combining Lemma 11 and Lemma 13. □

The proof of Lemma 5 is by induction. At the beginning, one has $0 \leqslant p^{\theta 0}(0) \leqslant 1$, thus $p^{\theta 0}_{\min}(0) = 0$ and $p^{\theta 0}_{\max}(0) = 1$. Using Lemma 14, one has $F_\theta(0,1) \leqslant F_\theta\left(p^{00}(0), p^{10}(0)\right) \leqslant F_\theta(1,0)$, thus

$$\begin{cases} p^{00}_{\min}(1) = F_0(0,1) = g(\beta) > 0 = p^{00}_{\min}(0), \\ p^{00}_{\max}(1) = F_0(1,0) = g(\alpha) < 1 = p^{00}_{\max}(0), \\ p^{10}_{\min}(1) = F_1(0,1) = g(\gamma) > 0 = p^{10}_{\min}(0), \\ p^{10}_{\max}(1) = F_1(1,0) = g(\beta) < 1 = p^{10}_{\max}(0), \end{cases} \tag{73}$$

thus (47) and (48) are true for $n = 1$.

Consider then an arbitrary $n \in \mathbb{N}^*$ and $n > 1$. Assume that (47) and (48) are satisfied for any $n' < n$ and $n' \in \mathbb{N}^*$, one needs to see whether (47) and (48) are still satisfied for n. Applying Lemma 14 again, one obtains

$$\begin{aligned} p^{\theta 0}_{\min}(n) &= F_\theta\left(p^{00}_{\min}(n-1), p^{10}_{\max}(n-1)\right) \\ &> F_\theta\left(p^{00}_{\min}(n-2), p^{10}_{\max}(n-2)\right) = p^{\theta 0}_{\min}(n-1), \end{aligned}$$

and

$$\begin{aligned} p^{\theta 0}_{\max}(n) &= F_\theta\left(p^{00}_{\max}(n-1), p^{10}_{\min}(n-1)\right) \\ &< F_\theta\left(p^{00}_{\max}(n-2), p^{10}_{\min}(n-2)\right) = p^{\theta 0}_{\max}(n-1), \end{aligned}$$

Similarly, one gets $p^{10}_{\min}(n) > p^{10}_{\min}(n-1)$ and $p^{\theta 0}_{\max}(n) < p^{\theta 0}_{\max}(n-1)$.

Appendix D
Proof of Proposition 6

As seen in the proof of Proposition 4, $\forall n \in \mathbb{N}^*$, $\mathbf{F}(\mathbf{p})$ maps $\mathcal{P}_n$ to $\mathcal{P}_n$, with $\mathcal{P}_n = \left[p^{00}_{\min}(n), p^{00}_{\max}(n)\right] \times \left[p^{10}_{\min}(n), p^{10}_{\max}(n)\right]$. In order to apply Banach's fixed-point theorem [29] to prove Proposition 6, it suffices to show that $\mathbf{F}$ is contracting, *i.e.*, that for any pairs $\mathbf{p} = (x,y) \in \mathcal{P}_n$ and $\mathbf{p} + \boldsymbol{\delta} = (x+\delta_x, y+\delta_y) \in \mathcal{P}_n$, one has

$$|\mathbf{F}(\mathbf{p}+\boldsymbol{\delta}) - \mathbf{F}(\mathbf{p})| < |\boldsymbol{\delta}|. \tag{74}$$

A sufficient condition to have (74) is that the eigenvalues of the matrix

$$\mathbf{A} = \begin{pmatrix} \frac{\partial F_0(x,y)}{\partial x} & \frac{\partial F_0(x,y)}{\partial y} \\ \frac{\partial F_1(x,y)}{\partial x} & \frac{\partial F_1(x,y)}{\partial y} \end{pmatrix}$$

have module less than 1. The eigenvalues of $\mathbf{A}$ are the solutions of

$$z^2 - \left(\frac{\partial F_0}{\partial x} + \frac{\partial F_1}{\partial y}\right) z + \left(\frac{\partial F_0}{\partial x}\frac{\partial F_1}{\partial y} - \frac{\partial F_0}{\partial y}\frac{\partial F_1}{\partial x}\right) = 0. \tag{75}$$

As in Appendix C, denote $\alpha = q_{\text{FA}}(2)$, $\beta = q_{\text{D}}(1,1)$ and $\gamma = q_{\text{D}}(0,2)$. First, one evaluates

$$\frac{\partial F_0}{\partial x}\frac{\partial F_1}{\partial y} - \frac{\partial F_0}{\partial y}\frac{\partial F_1}{\partial x} = \frac{\partial g}{\partial h_0}\frac{\partial g}{\partial h_1}\left(\frac{\partial h_0}{\partial x}\frac{\partial h_1}{\partial y} - \frac{\partial h_0}{\partial y}\frac{\partial h_1}{\partial x}\right) \overset{(a)}{=} 0,$$

where (a) comes from $\frac{\partial h_0}{\partial x}\frac{\partial h_1}{\partial y} = \frac{\partial h_0}{\partial y}\frac{\partial h_1}{\partial x}$, using the partial derivatives calculated in the proof of Lemma 11. Then, the solutions of (75) are $z_1 = \frac{\partial F_0}{\partial x} + \frac{\partial F_1}{\partial y}$ and $z_2 = 0$. Hence, it suffices to prove that $|z_1| < 1$.

We begin with the evaluation of an upper bound of the partial derivative of $F_0(x,y)$ with respect to x

$$\begin{aligned} \frac{\partial F_0(x,y)}{\partial x} &= \frac{\partial g(h_0(x,y))}{\partial x} = \frac{\partial g}{\partial h_0}\cdot\frac{\partial h_0}{\partial x} \\ &\overset{(a)}{=} \frac{(\beta-\alpha)p_0p_1y}{(p_0x+p_1y)^2}\sum_{i:i/M<\nu}\binom{M}{i}h_0^i(1-h_0)^{M-i}\frac{h_0M-i}{h_0(1-h_0)} \\ &\overset{(b)}{\leqslant} \frac{(\beta-\alpha)p_0p_1y}{(p_0x+p_1y)^2}F_0(x,y)\frac{M}{1-h_0} \leqslant c_0(\alpha,\beta,\gamma,M,\nu,n), \end{aligned} \tag{76}$$

where (a) is obtained using (70), (b) comes from $i \geqslant 0$, and c_0 is defined in (44). Meanwhile, from Lemma 14, one has $\partial F_0(x,y)/\partial x \geqslant 0$, as F_0 is an increasing function of x.

Similarly,

$$\begin{aligned} \frac{\partial F_1(x,y)}{\partial y} &= \frac{\partial g(h_1(x,y))}{\partial y} = \frac{\partial g}{\partial h_1}\cdot\frac{\partial h_1}{\partial y} \\ &= \frac{(\gamma-\beta)p_0p_1x}{(p_0x+p_1y)^2}\sum_{i:i/M<\nu}\binom{M}{i}h_1^i(1-h_1)^{M-i}\frac{i-h_1M}{h_1(1-h_1)} \\ &\geqslant \frac{(\gamma-\beta)p_0p_1x}{(p_0x+p_1y)^2}F_1(x,y)\frac{-M}{1-h_1} \geqslant -c_1(\alpha,\beta,\gamma,M,\nu,n), \end{aligned} \tag{77}$$

and $\partial F_1(x,y)/\partial y \leqslant 0$ as F_1 is a non-decreasing function of y. One concludes that

$$-c_1 \leqslant \frac{\partial F_0(x,y)}{\partial x} + \frac{\partial F_1(x,y)}{\partial y} \leqslant c_0,$$

thus $c_0 < 1$ and $c_1 < 1$ lead to $|z_1| < 1$, which ensures the unicity of the equilibrium.

Appendix E
Proof of Proposition 8

First, one shows that if $\nu < q_{\text{D}}(1,1)$, then for any $\varepsilon > 0$, there exists $M > M'$, such that $\overline{p}^{10} < \varepsilon$.

From Lemma 5, $\overline{p}^{10}$ can be bounded as

$$\begin{aligned} \overline{p}^{10} &= F_1\left(\overline{p}^{00}, \overline{p}^{10}\right) \\ &< \sum_{k:k/M<\nu}\binom{M}{k}\left(q_{\text{D}}(1,1)\right)^k\left(1-q_{\text{D}}(1,1)\right)^{M-k} \end{aligned} \tag{78}$$

Consider $\Phi_1, \Phi_2, \ldots$ an infinite sequence of *i.i.d.* binary random variables with $\mathbb{P}\{\Phi_m = 1\} = q_{\text{D}}(1,1)$. For any $\varrho \in [0,1]$ such that $\varrho M \in \mathbb{N}^+$, one has

$$\mathbb{P}\left\{\frac{\sum_{m=1}^M \Phi_m}{M} = \varrho\right\} = \binom{M}{\varrho M}\left(q_{\text{D}}(1,1)\right)^{\varrho M}\left(1-q_{\text{D}}(1,1)\right)^{M(1-\varrho)}.$$

According to the weak law of large numbers [33], for $\varepsilon > 0$, there exists M', such that for any $M > M'$, one has

$$\mathbb{P}\left\{\left|\frac{\sum_{m=1}^M \Phi_m}{M} - q_{\text{D}}(1,1)\right| > q_{\text{D}}(1,1)\right\} < \varepsilon. \tag{79}$$

From (79), one also has

$$\begin{aligned} &\sum_{k:k/M<(q_{\text{D}}(1,1)-\varepsilon)}\left(q_{\text{D}}(1,1)\right)^k\left(1-q_{\text{D}}(1,1)\right)^{M-k} \\ &= \mathbb{P}\left\{\frac{\sum_{m=1}^M \Phi_m}{M} - q_{\text{D}}(1,1) < -\varepsilon\right\} \leqslant \mathbb{P}\left\{\left|\frac{\sum_{m=1}^M \Phi_m}{M} - q_{\text{D}}(1,1)\right| > \varepsilon\right\} \\ &< \varepsilon. \end{aligned} \tag{80}$$

If $\nu < q_{\mathrm{D}}(1,1) - \varepsilon$, then using (80), the bound of $\overline{p}^{10}$ in (78) may be further written as

$$\begin{aligned}\overline{p}^{10} &< \sum_{k:k/M<\nu} \binom{M}{k} \left(q_{\mathrm{D}}(1,1)\right)^k \left(1-q_{\mathrm{D}}(1,1)\right)^{M-k} \\ &\leqslant \sum_{k:k/M<(q_{\mathrm{D}}(1,1)-\varepsilon)} \left(q_{\mathrm{D}}(1,1)\right)^k \left(1-q_{\mathrm{D}}(1,1)\right)^{M-k} < \varepsilon. \end{aligned} \tag{81}$$

From Lemma 11 and the fact that $q_{\mathrm{FA}}(2) \leqslant \overline{p}^{10} \leqslant q_{\mathrm{D}}(1,1)$ and $0 \leqslant \overline{p}^{10} < \varepsilon$, one has $h_0\left(\overline{p}^{00}, \overline{p}^{10}\right) \in [q_{\mathrm{FA}}(2), \chi(\varepsilon)]$, with

$$\chi(\varepsilon) = \frac{p_0 \left(q_{\mathrm{FA}}(2)\right)^2 + p_1 q_{\mathrm{D}}(1,1)\,\varepsilon}{p_0 q_{\mathrm{FA}}(2) + p_1 \varepsilon}. \tag{82}$$

Thus, according to Lemma 13,

$$\begin{aligned}&\overline{p}^{00} = F_0\left(\overline{p}^{00}, \overline{p}^{10}\right) = g\left(h_0\left(\overline{p}^{00}, \overline{p}^{10}\right)\right) \\ &\geqslant g(\chi(\varepsilon)) = \sum_{k:k/M<\nu} \binom{M}{k} \left(\chi(\varepsilon)\right)^k \left(1-\chi(\varepsilon)\right)^{M-k}. \end{aligned} \tag{83}$$

Using derivations similar to those leading to (80), one gets

$$\sum_{k:k/M>(\chi(\varepsilon)+\varepsilon)} \binom{M}{k} \left(\chi(\varepsilon)\right)^k \left(1-\chi(\varepsilon)\right)^{M-k} < \varepsilon, \tag{84}$$

which leads to

$$\sum_{k:k/M\leqslant(\chi(\varepsilon)+\varepsilon)} \binom{M}{k} \left(\chi(\varepsilon)\right)^k \left(1-\chi(\varepsilon)\right)^{M-k} \geqslant 1-\varepsilon. \tag{85}$$

If $\nu > \chi(\varepsilon) + \varepsilon$, then

$$\begin{aligned}\overline{p}^{00} &\geqslant \sum_{k:k/M<\nu} \binom{M}{k} \left(\chi(\varepsilon)\right)^k \left(1-\chi(\varepsilon)\right)^{M-k} \\ &\geqslant \sum_{k:k/M\leqslant(\chi(\varepsilon)+\varepsilon)} \left(\chi(\varepsilon)\right)^k \left(1-\chi(\varepsilon)\right)^{M-k} \geqslant 1-\varepsilon. \end{aligned} \tag{86}$$

As a conclusion, for any $\varepsilon > 0$, if $\chi(\varepsilon) + \varepsilon < \nu < q_{\mathrm{D}}(1,1) - \varepsilon$, then $\overline{p}^{00} \geqslant 1-\varepsilon$ and $\overline{p}^{10} < \varepsilon$. Since $\lim_{\varepsilon\to 0} \chi(\varepsilon) = q_{\mathrm{FA}}(2)$, one concludes that if $q_{\mathrm{FA}}(2) < \nu < q_{\mathrm{D}}(1,1)$, one obtains (50).

REFERENCES

[1] M. J. Khabbaz, C. M. Assi, and W. F. Fawaz, "Disruption-tolerant networking: A comprehensive survey on recent developments and persisting challenges," *IEEE Communications Surveys & Tutorials*, vol. 14, no. 2, pp. 607–640, 2012.

[2] P. R. Pereira, A. Casaca, J. J. Rodrigues, V. N. Soares, J. Triay, and C. Cervelló-Pastor, "From delay-tolerant networks to vehicular delay-tolerant networks," *IEEE Communications Surveys & Tutorials*, vol. 14, no. 4, pp. 1166–1182, 2012.

[3] P. Hui, J. Crowcroft, and E. Yoneki, "Bubble rap: Social-based forwarding in delay-tolerant networks," *IEEE Trans. on Mobile Computing*, vol. 10, no. 11, pp. 1576–1589, 2011.

[4] V. N. Soares, J. J. Rodrigues, and F. Farahmand, "Geospray: A geographic routing protocol for vehicular delay-tolerant networks," *Information Fusion*, vol. 15, pp. 102–113, 2014.

[5] H. Zhu, S. Du, Z. Gao, M. Dong, and Z. Cao, "A probabilistic misbehavior detection scheme toward efficient trust establishment in delay-tolerant networks," *IEEE Trans. on Parallel and Distributed Systems*, vol. 25, no. 1, pp. 22–32, 2014.

[6] L. Galluccio, B. Lorenzo, and S. Glisic, "Sociality-aided new adaptive infection recovery schemes for multicast dtns," *IEEE Trans. on Vehicular Technology*, vol. PP, no. 99, pp. 1–1, 2015.

[7] M. Panda, A. Ali, T. Chahed, and E. Altman, "Tracking message spread in mobile delay tolerant networks," *IEEE Trans. on Mobile Computing*, vol. 14, no. 8, pp. 1737–1750, 2015.

[8] W. Li, F. Bassi, D. Dardari, M. Kieffer, and G. Pasolini", "Defective sensor identification for WSNs involving generic local outlier detection tests," *IEEE Trans. on Signal and Information Processing over Networks*, vol. 2, no. 1, pp. 29–48, 2016.

[9] Y. Zhang, N. Meratnia, and P. Havinga, "Outlier detection techniques for wireless sensor networks: A survey," *IEEE Communications Surveys & Tutorials*, vol. 12, no. 2, pp. 159–170, 2010.

[10] A. Mahapatro and P. M. Khilar, "Fault diagnosis in wireless sensor networks: A survey," *IEEE Communications Surveys & Tutorials*, vol. 15, no. 4, pp. 2000–2026, 2013.

[11] H. Dong, Z. Wang, S. X. Ding, and H. Gao, "A survey on distributed filtering and fault detection for sensor networks," *Mathematical Problems in Engineering*, 2014.

[12] J. Chen, S. Kher, and A. Somani, "Distributed fault detection of wireless sensor networks," in *Proc Workshop DIWANS*, New York, NY, 2006, pp. 65 – 72.

[13] J.-L. Gao, Y.-J. Xu, and X.-W. Li, "Weighted-median based distributed fault detection for wireless sensor networks," *Journal of Software*, vol. 18, no. 5, pp. 1208 – 1217, 2007.

[14] S. Ji, S.-F. Yuan, T.-H. Ma, and C. Tan, "Distributed fault detection for wireless sensor based on weighted average," in *Proc NSWCTC*, Wuhan, China, 2010, pp. 57 – 60.

[15] M. Panda and P. Khilar, "Distributed self fault diagnosis algorithm for large scale wireless sensor networks using modified three sigma edit test," *Ad Hoc Networks*, vol. 25, pp. 170–184, 2015.

[16] B. Zhu, W. Zhang, W. Feng, and L. Zhang, "Distributed faulty node detection and isolation in delay-tolerant vehicular sensor networks," in *Proc. PIMRC*, Sept 2012, pp. 1497–1502.

[17] W. Peng, F. Li, X. Zou, and J. Wu, "Behavioral malware detection in delay tolerant networks," *IEEE Trans. on Parallel and Distributed Systems*, vol. 25, no. 1, pp. 53–63, 2014.

[18] E. Hernandez-Orallo, M. D. Serrat Olmos, J.-C. Cano, C. T. Calafate, and P. Manzoni, "Cocowa: A collaborative contact-based watchdog for detecting selfish nodes," *IEEE Trans. on Mobile Computing*, vol. 14, no. 6, pp. 1162–1175, 2015.

[19] E. Ayday and F. Fekri, "An iterative algorithm for trust management and adversary detection for delay-tolerant networks," *IEEE Trans. on Mobile Computing*, vol. 11, no. 9, pp. 1514–1531, 2012.

[20] Y. Liu, D. R. Bild, R. P. Dick, Z. M. Mao, and D. S. Wallach, "The mason test: A defense against sybil attacks in wireless networks without trusted authorities," *IEEE Trans. on Mobile Computing*, vol. 14, no. 11, pp. 2376–2391, 2015.

[21] J. R. Douceur, "The sybil attack," in *Peer-to-peer Systems*. Springer, 2002, pp. 251–260.

[22] G. Han, J. Jiang, L. Shu, and M. Guizani, "An attack-resistant trust model based on multidimensional trust metrics in underwater acoustic sensor network," *IEEE Trans. on Mobile Computing*, vol. 14, no. 12, pp. 2447–2459, 2015.

[23] H. Zhu, L. Fu, G. Xue, Y. Zhu, M. Li, and L. Ni, "Recognizing exponential inter-contact time in vanets," in *Proc. INFOCOM*, March 2010, pp. 1–5.

[24] J. P. Norton, Ed., Special Issue on Bounded-Error Estimation: Issue 1, 1994, *Int. Jnl of Adapt. Cont. and Sig. Proc.* **8**(1):1–118.

[25] ——, Special Issue on Bounded-Error Estimation: Issue 2, 1995, *Int. Jnl of Adapt. Cont. and Sig. Proc.* **9**(1):1–132.

[26] M. Milanese, J. Norton, H. Piet-Lahanier, and E. Walter, Eds., *Bounding Approaches to System Identification*. New York, NY: Plenum Press, 1996.

[27] L. Jaulin, M. Kieffer, O. Didrit, and E. Walter, *Applied Interval Analysis*. London: Springer-Verlag, 2001.

[28] A. Granas and J. Dugundji, *Fixed point theory*. Springer Science & Business Media, 2013.

[29] S. Banach, "Sur les opérations dans les ensembles abstraits et leur application aux équations intégrales," *Fund. Math.*, vol. 3, no. 1, pp. 133–181, 1922.

[30] N. Eagle and A. Pentland, "Reality mining: sensing complex social systems," *Personal and ubiquitous computing*, vol. 10, no. 4, pp. 255–268, 2006.

[31] J. Scott, R. Gass, J. Crowcroft, P. Hui, C. Diot, and A. Chaintreau, "CRAWDAD dataset cambridge/haggle (v. 2009-05-29)," Downloaded from http://crawdad.org/cambridge/haggle/20090529, May 2009.

[32] M. Orlinski, "Encounter traces for the one simulator," Downloaded from http://www.shigs.co.uk/index.php?page=traces.

[33] T. M. Cover and J. A. Thomas, *Elements of information theory*. John Wiley & Sons, 2012.